POST RETROFIT ANALYSIS OF THE TUTTLE CREEK BRIDGE
Br. No. 16-81-2.24

By

Benjamin Anderson
Stanley T. Rolfe
Adolfo B. Matamoros.
Caroline Bennett
Santiago Bonetti

A Report on Research Sponsored by

Structural Engineering and Engineering Materials
SM Report No. 88
January 2007

THE UNIVERSITY OF KANSAS CENTER FOR RESEARCH, INC
LAWRENCE, KANSAS

ABSTRACT

The Tuttle Creek Bridge was built in 1962. Like many older welded steel bridges, it has developed fatigue cracks. The majority of cracks were forming in the upper web-gap region. In addition, fatigue cracking was occurring along gusset plates in the structure. A retrofit was performed in 1986 to prevent further fatigue cracking. Unfortunately, the cracks propagated after the retrofit. Therefore, finite element models were created at the University of Kansas to investigate the continued fatigue cracking. The models supplied a more effective retrofit procedure that included attaching the connection stiffener to the upper flange of the girder.

Two tests were planned to determine the effectiveness of the retrofit. The first field test occurred before the repair was started. Its purpose was to provide stress values in key areas for comparison after the repair. In addition, the pre-retrofit test provided information for future finite element models. In 2005, the second retrofit was completed.

The purpose of this report is to present results of the post-retrofit test with data from the pre-retrofit test. Comparisons of stresses for each key area are included in the report. Details of the Tuttle Creek Bridge and testing procedure are provided. In addition, minor changes from the previous test are described.

ACKNOWLEDGEMENTS

TABLE OF CONTENTS

LIST OF FIGURES

LIST OF TABLES

CHAPTER 1   INTRODUCTION

The Tuttle Creek Bridge was built in 1962 as a means of crossing the Tuttle Creek Reservoir. It is a two-girder steel bridge that consists of 30 spans that total 5350 ft in length. The width of the deck consists of two 12 ft lanes with 2 ft shoulders on each side. The cross section of the width can be seen in Figure 1-1. Profile and plan views can be seen in Figures 1-2 and 1-3, respectively. The bridge is located in the northern region of Kansas near the town of Randolph. This region does not have a high amount of traffic, with approximately 520 vehicles per day crossing the bridge. In addition, the region is relatively flat and the bridge is exposed to high wind conditions.

The Tuttle Creek Bridge developed fatigue cracking in the super-structure. This fatigue cracking was a potential threat to the longevity of the bridge. Because the bridge was designed with very little redundancy, the structure was considered fracture critical. A failure of any one of the structural members could result in a failure of some portion of the structure.

The fatigue cracking was located in two types of connections. The first location was in the web-gap region located at each diaphragm. The web-gap region is found between the fillet weld of the flange/web connection and the top of the connection stiffener. The second location was in the welds attaching the lateral gusset plate to the bottom flange of the beam. Repairs were completed at both types of crack locations in 1986. In the case of the web-gap region, the repairs proved to be ineffective. Repair methods were successful for the lateral gusset plates in which they were implemented. However, plates that were not repaired developed cracks at a later time.

A finite element model of the web-gap region of the bridge was developed at the University of Kansas in 2000. Dr. Yuan Zhao, a former KU graduate student, investigated the connection and the efficiency of potential retrofit procedures. A retrofit procedure was implemented in 2005, based on the results of the model.

To verify the results from the finite element model and the effect of the repairs, two sets of field measurements investigations were completed. The first investigation, performed prior to the retrofit, provided the means to compare measured results to those from the finite element model. In addition, this study investigated other fatigue-prone details, such as the connection between the gusset plates and the longitudinal stiffeners. Information gathered from these connections will be used to improve future finite element models. The second investigation was performed after the retrofit measures had been completed. The methodology from the first investigation was followed as closely as possible to provide an accurate comparison.

This report addresses the results of the second field investigation. The focus of this report will be the comparison between the two field investigations. Since this report focuses on the comparison between the field investigations, pertinent information from the first field report (Marshall et al., 2005) are included in this report. In addition, an effort was made to maintain continuity between the pre-retrofit report and the post-retrofit report. For the locations that remained the same for both investigations, a direct comparison in stress values is presented. Results for the other locations are provided also.
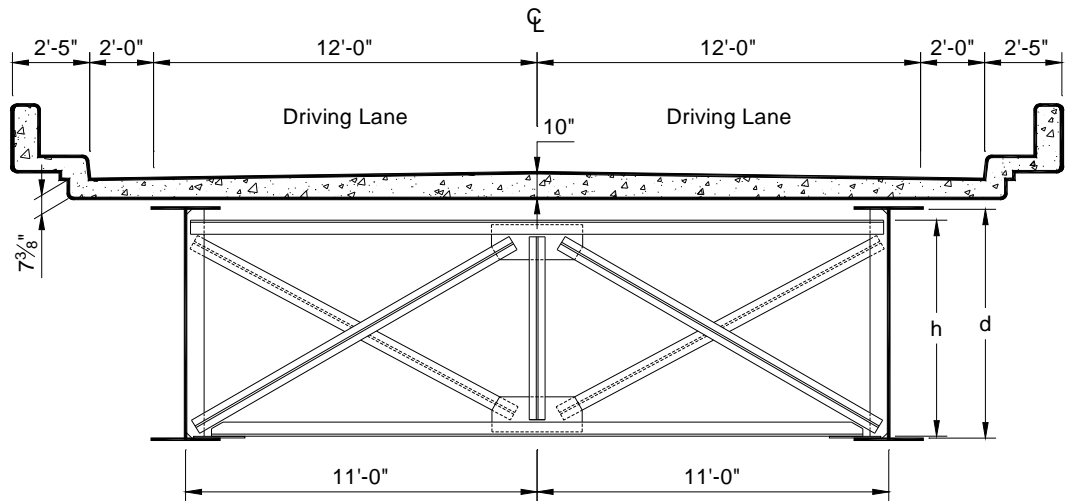
Figure 1-1: Tuttle Creek Bridge Cross Section
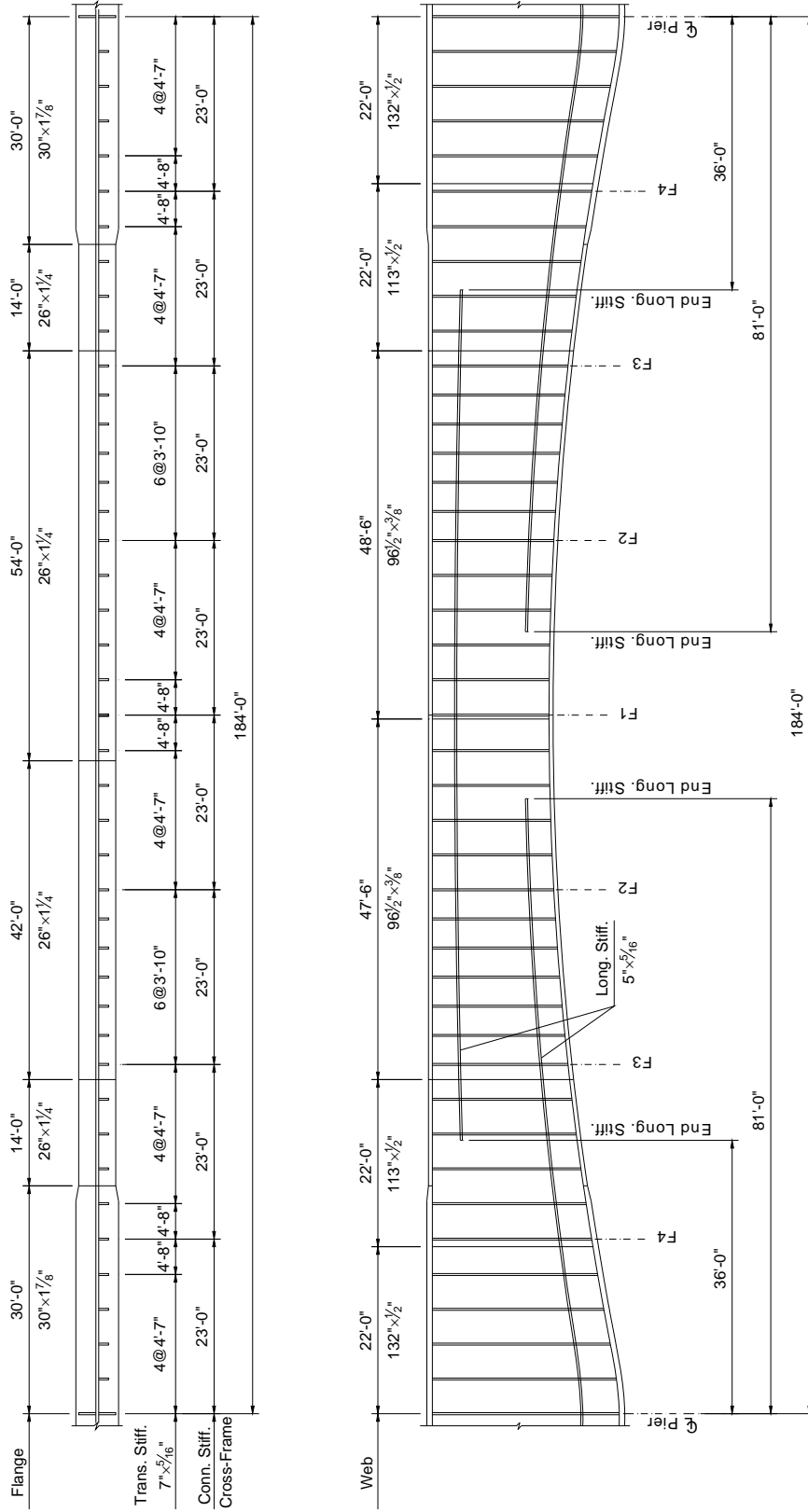
Figure 1-2: Girder Details of Typical Intermediate Spans for Tuttle Creek Bridge
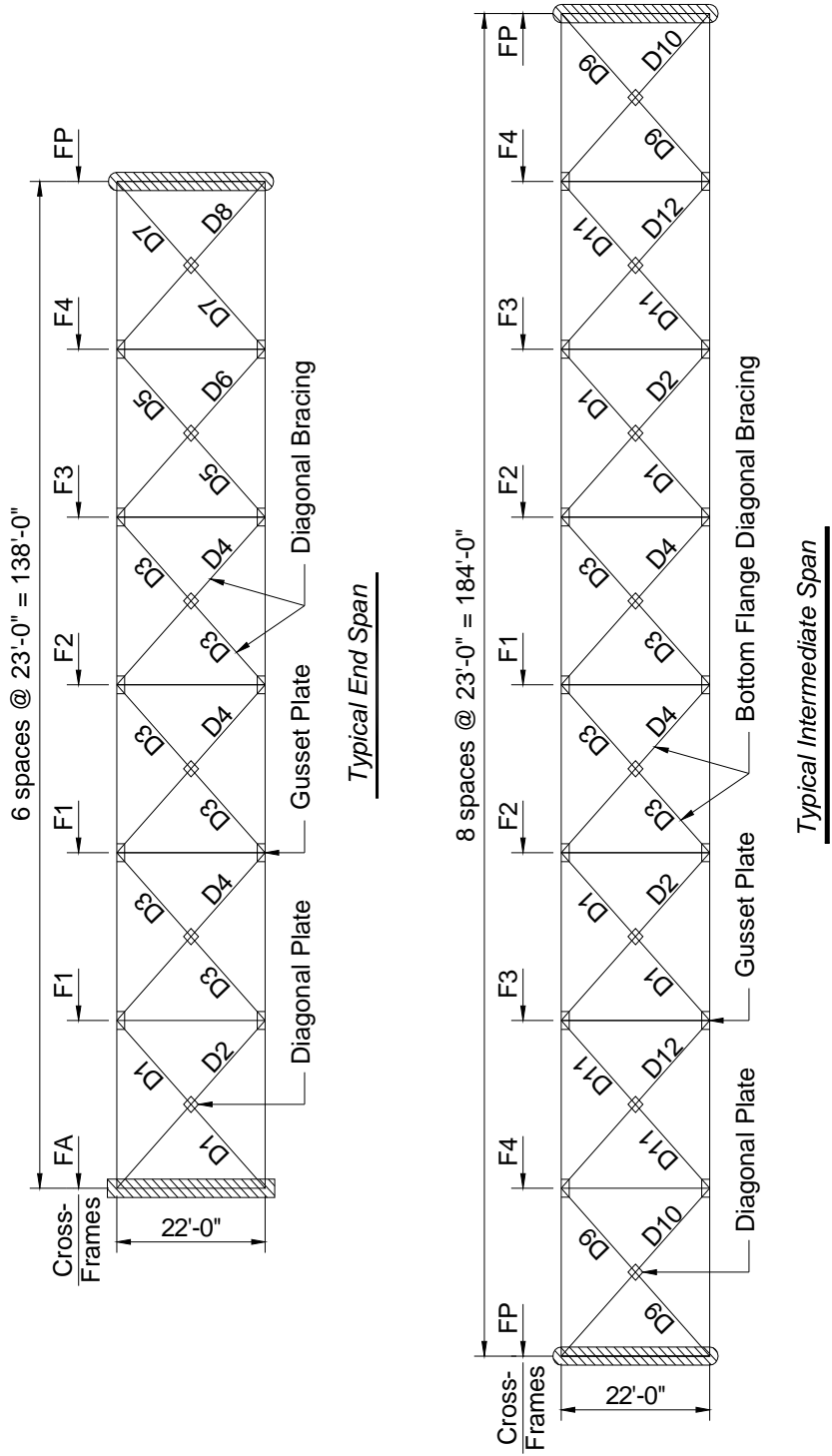
Figure 1-3 Tuttle Creek Bridge Framing Plan

5

CHAPTER 2   FATIGUE HISTORY

The significance of fatigue-prone details was not completely understood when the Tuttle Creek Bridge was designed. In particular, distortion-induced fatigue cracking was overlooked. Differential deflection between the two girders creates high secondary stresses, which can lead to fatigue cracking. The locations investigated due to high stress concentrations included the web gap region, along the gusset plate, and at the end of the longitudinal stiffener.

In addition to repairs performed in those locations, other repair procedures were completed. These included replacement of the pin and hanger system, repair of web field splices, and ultrasonic impact treatment (UIT) of the welds. The effects of these procedures are outside the scope of this report, but information about the ultrasonic impact treatment of welds is provided in Appendix A.

2.1   Web-Gap Cracking

The web gap region consisted of a 1"x 1" diagonal cut removed from the top and bottom of the stiffener as shown in Figures 2-1 and 2-2. This cut allowed the fillet weld between the web and flange to be continuous. This gap creates high stress concentrations in the web and creates the potential for fatigue cracks to propagate in this area. Two types of cracks that occurred in the upper web-gap region were designated as either weld tears or horizontal cracks. Figure 2-3 shows the two types of cracks, and Figure 2-4 presents a photograph of actual cracks.

2.1.1   Cracking Patterns

Of the two types of cracking, weld tears were found to be the most common. The weld tears propagated down the 4 in. fillet weld between the upper portion of the stiffener and the web. Many of the 4 in. top intermittent welds on the stiffener were broken completely by weld tears. In addition, some weld tears propagated from the fillet weld into the web of the girder.

6

The other cracking pattern found in the web gap region was horizontal cracking. The horizontal cracks occurred at the base of the fillet weld that connects the upper flange to the web. Horizontal cracks were located mainly on the interior side of the girders, but were also found on the exterior side.

2.1.2 Source of Cracking

The primary source of fatigue cracking in the Tuttle Creek Bridge was the lack of attachment between the top of the stiffener and the tension flange. The web-gap cracking was the result of differential deflection of the girders. Braces in the diaphragms created a tension force on the stiffener due to the difference in deflections between the two girders. This caused the web-gap to undergo double-curvature bending. Figure 2-5 shows the tension force created by the diaphragms. This type of detail is classified as a category C fatigue detail according to the 2004 AASHTO LFRD specifications.

Because the cracks were caused by forces induced by the diaphragms, web-gap cracking only occurred at diaphragm locations along the girder. Two web-gap regions are located at the top and bottom of the stiffener, at each diaphragm connection. For the Tuttle Creek Bridge, web-gap cracks were found exclusively in the upper regions. This was a result of the relative flexibility of the lower flange compared to the upper flange. The concrete decking rigidly held the upper flange while the lower flange had no such restraint. Because the lower flange was not restrained from rotating, the stresses developed were not as high as the stresses in the upper flange. Thus, cracks were found only in the upper flange.

2.1.3 Crack Repairs

A previous repair of the web-gap region was implemented in 1986. To repair the weld tears, the joint was "softened" by cutting the stiffeners 1 in. below the termination of the existing cracks. A 0.5-in. radius was placed at the end of the cut. Even though this was supposed to have repaired the problem, weld tears continued to

grow in this region. To stop the horizontal cracks, 0.75 in. diameter stop holes were drilled at the tips of existing cracks. However, the horizontal cracks reinitiated after the retrofit.

To determine a new retrofit strategy, the Kansas Department of Transportation (KDOT) requested a study of the web-gap region to be completed by KU. Dr. Yuan Zhao, a former KU graduate student, created finite element models of the web-gap region for the Tuttle Creek Bridge (Zhao et al., 2003). Based on the analysis, it was determined that a positive connection between the connection stiffener and the flange would provide improved performance. The investigation is summarized in Appendix B.

2.2   Gusset Plate Cracking

Fatigue cracking also occurred in the fillet weld between the gusset plate and the lower flange of the girder. Gusset plates connect the girders to the lateral bracing of the girders. As shown in Figure 2-7, three structural tees enter the connection. Loads imposed by the lateral bracing caused cracking of the gusset plate connection.

In addition to fatigue related cracks, several tack welds on the underside of the gusset plate, where it overhangs the girder, were found to have broken. Because the tack welds were not essential to the structural integrity of the bridge, a problem arises only if cracks extend into the lower flange. If a crack were to develop in the tension flange, significant crack growth could occur due to the primary loading of the bridge.

2.2.1   Cracking Patterns

Cracks developed in welds that were both perpendicular and parallel to the gusset plate. Figure 2-6 shows a drawing of the cracking patterns, while Figure 2-7 displays an actual fillet weld crack.

The more common of the two was the cracking of the fillet weld perpendicular to the gusset plate. The fillet welds extended symmetrically across the back six inches along the sides of the gusset plate. This type of detail is classified as a Category E

detail according to the 2004 AASHTO Bridge Specifications. The cracks are found at the end of the weld along the sides of the plate. The cracks were assumed to be only in the weld material, but could potentially propagate into the lower tension flange.

2.2.2 Sources of Cracking

The source of the gusset plate cracks was not clearly defined. One theory was that cracks developed from the bending stress of the girder (Figure 2-8). Another possibility considered was that distortion of the girder caused high compressive stresses in the diagonal bracing. The lateral bracing could potentially buckle upward along its weak axis introducing a prying action on the gusset plate (Figure 2-9). Another theory considered racking of the gusset plate due to loads from the diagonal bracing. Twisting of the gusset plate would cause cracking to develop at the ends of the fillet weld (Figure 2-10). To help clarify this issue, strain gages were placed on the top and the bottom of the plate as shown in Figure 2-11.

2.3 Longitudinal Stiffener Cracking

Longitudinal web stiffeners were used in regions of high compressive stresses. Stiffeners were located in the compressive region of both the positive and negative moment regions. The negative moment stiffeners extended symmetrically 81 ft from each pier, while positive moment stiffeners extended 56 ft symmetrically about the centerline of typical spans.

2.3.1 Cracking Pattern

Cracks had developed in the butt welds of the stiffener splices. The cracks are found only in the weld material. Figure 2-12 shows a crack in the longitudinal stiffener.

2.3.2 Source of Cracking

The crack was probably generated from a defect in the weld. Due to the bending of the girder, stress cycles occurred within the stiffener. These cycles propagated the crack in the stiffener.

Detail A
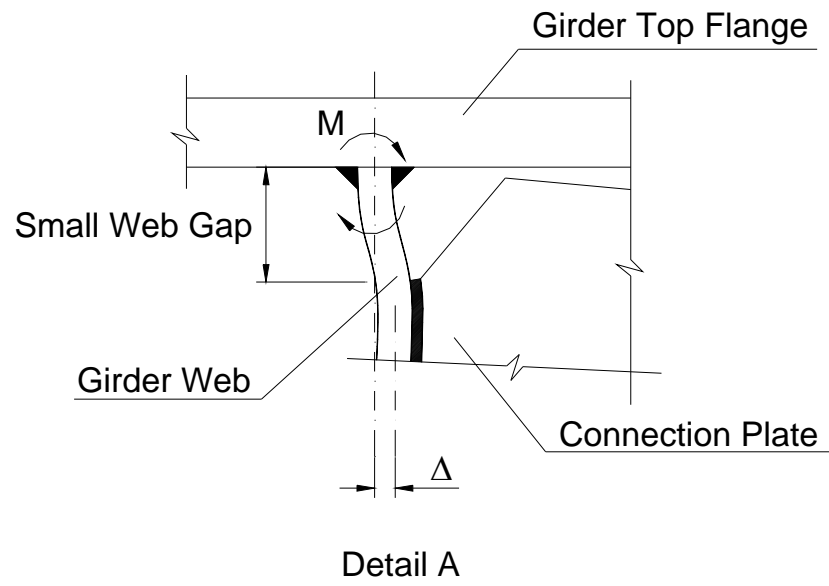
Figure 2-1: Web-Gap Region

Figure 2-2: Web-Gap Region (Picture)
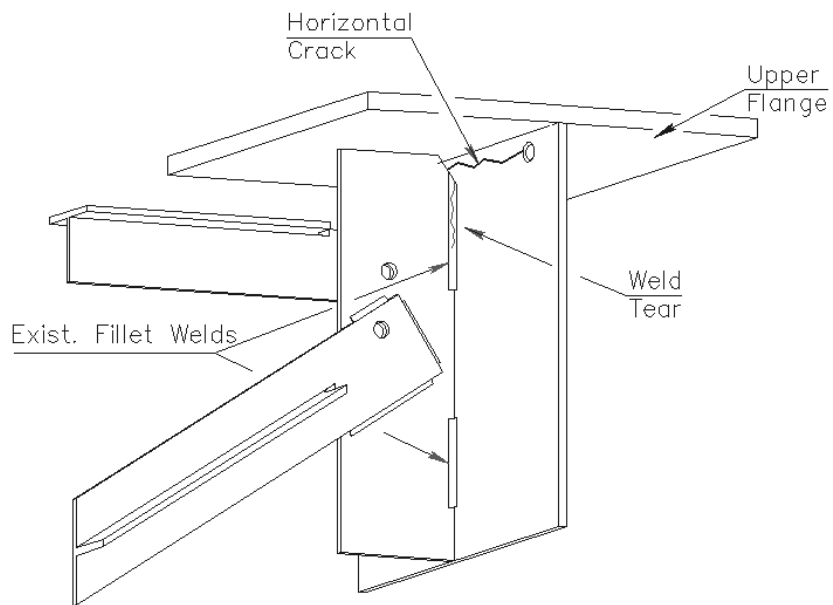
Figure 2-3: Web-Gap Cracking Patterns

Figure 2-4: Web-Gap Cracking Patterns (Picture)
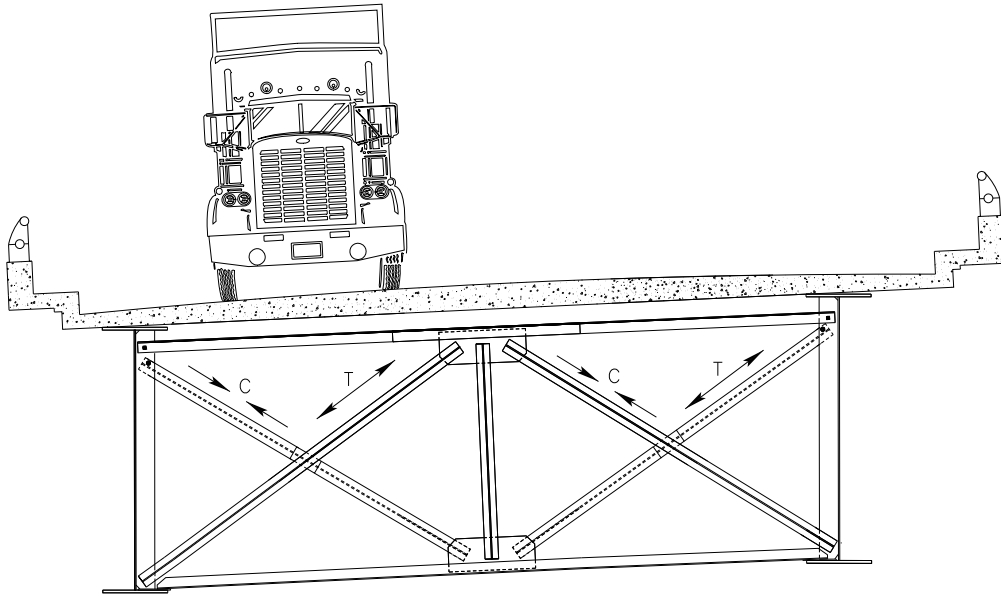
Figure 2-5: Differential Deflection of Girders
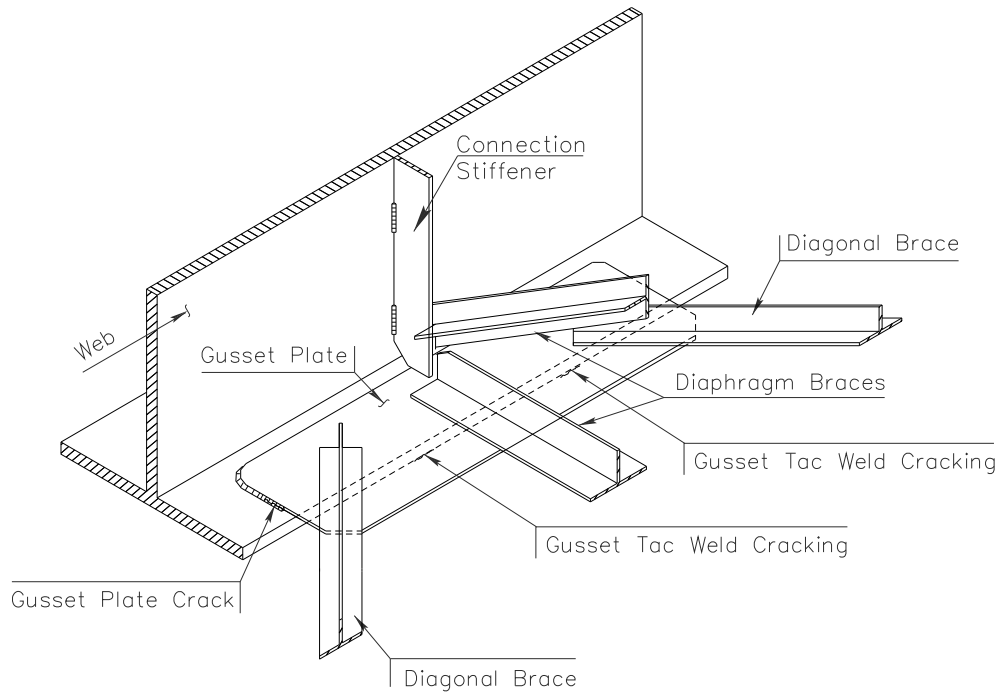
Figure 2-6: Gusset Plate Cracking Patterns

Figure 2-7: Gusset Plate Cracking Patterns (Picture)
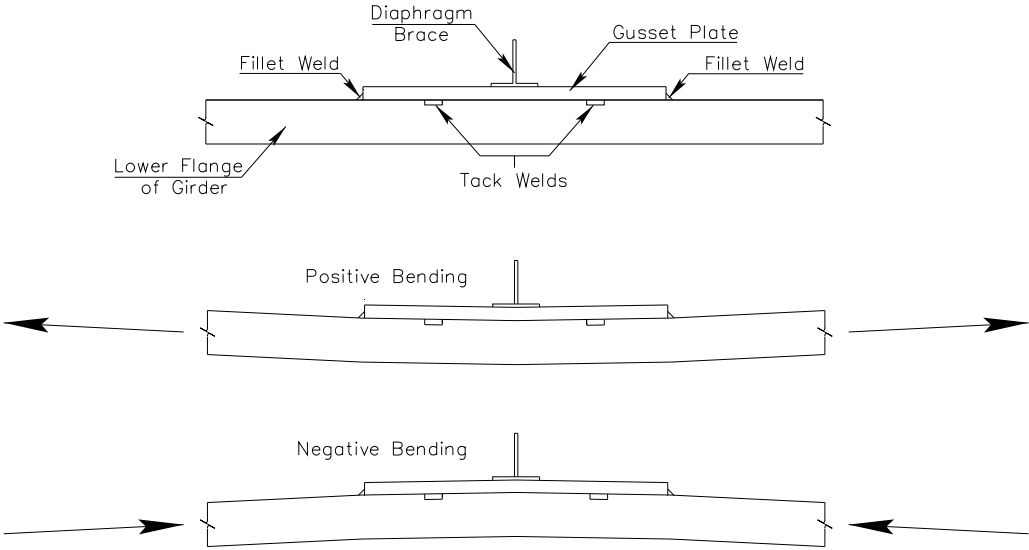
Figure 2-8: Gusset Plate Cracking Source (Bending Stresses)

14
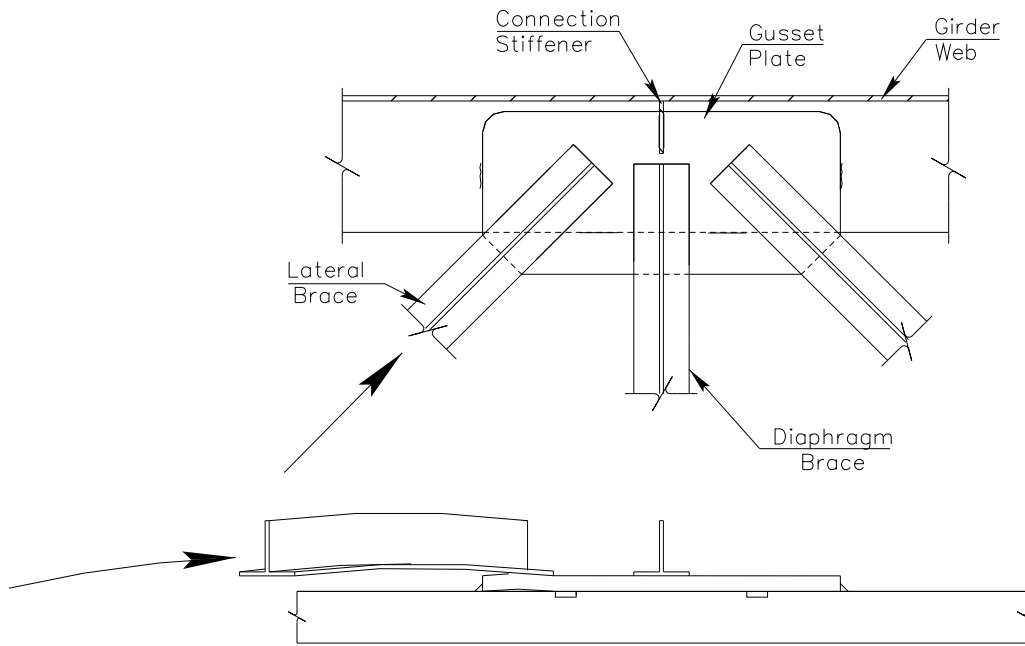
Figure 2-9: Gusset Plate Cracking Source (Distortion of Lateral Brace)
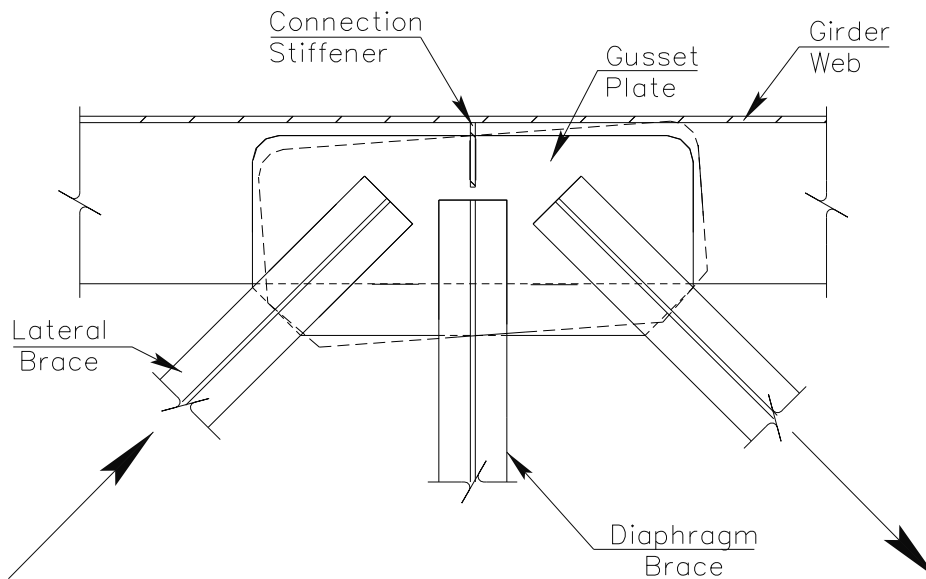
Figure 2-10: Gusset Plate Cracking Source (Racking of Gusset Plate)
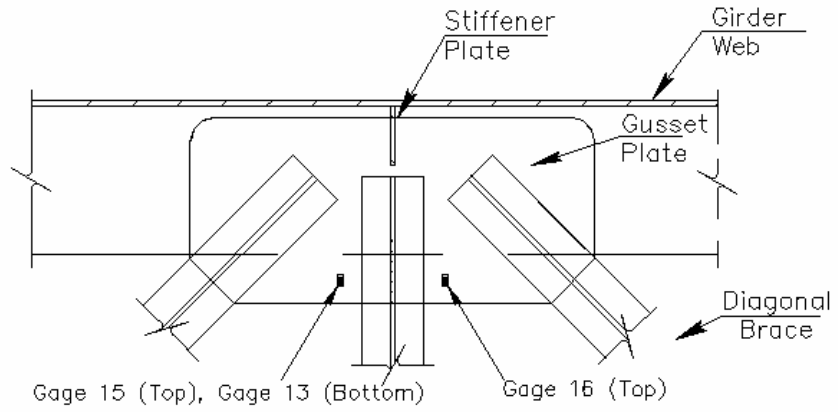
Figure 2-11: Relocated Strain Gages
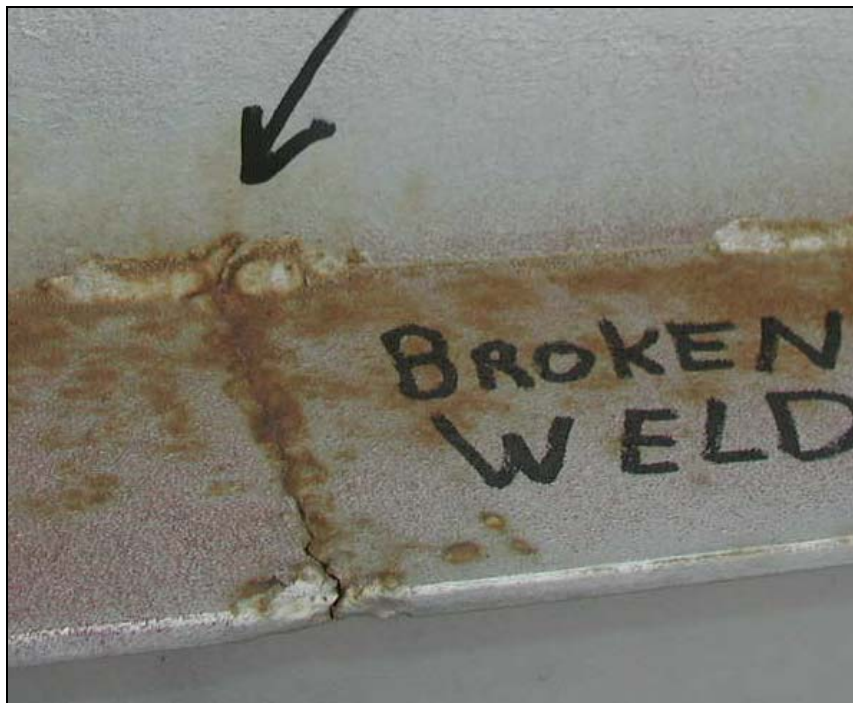
Figure 2-12: Longitudinal Stiffener Crack

CHAPTER 3   INSTALLATION & TESTING

To maintain continuity between the pre-retrofit and post-retrofit field measurements, the pre-retrofit installation and testing procedure was followed as closely as possible. When possible, strain gages were placed at the same locations as in the pre-retrofit test. Gages were placed again in span 29 in the web-gap region and on the longitudinal stiffener. Due to repairs, a few changes to the procedure were necessary. First, the gusset plate that was tested pre-retrofit had been replaced during the repair. Because the new plate was vastly different, the decision was made to move the gusset plate gages to span 28, on which the particular gusset plate had not been replaced. Second, five gages were added due to discovery of an unforeseen crack location. The results of the five added gages are presented in detail in Appendix E. Because the crack was located near span 14, the data acquisition system had to be moved during the testing. The result was that more than the maximum number of channels (23) could be used. Therefore, data was collected for 28 gages. Lastly, because no changes were made to the bracing, three of the bracing gages were relocated to the gusset plate. The gages were placed on the gusset plate to check for bending in the perpendicular direction to investigate sources of gusset plate cracking.

3.1 Test Preparation

In addition to reviewing previous test methods, the data collection equipment was checked before testing began. Supplies were prepared prior to the test. Gages were taped to a plastic sheet to prepare them for application. Full details of the testing procedure are listed in Appendix C.

3.2 Instrument Installation

Installation of the instruments was accomplished by using a snooper provided by KDOT. The snooper, which was operated by KDOT personnel, was able to

maneuver through the bracing and reach remote areas on the bridge. The snooper boom, shown in Figure 3-1, had one basket that was large enough for three people.

Along with providing the snooper, KDOT also provided traffic control for the installation. Two trucks were stationed at each end of the snooper during installation. Personnel for the gage installation included: two snooper operators, two gage installers, and four traffic control experts.

Installation of the gages was completed within three days. In addition to installing gages, work performed also included placing the wires underneath the bridge. On the third day, the data acquisition system was moved between all three piers to test the installed gages. Figure 3-2 displays the testing station mounted under the bridge. Further details of instrument installation and data acquisition setup can be found in Appendix C of this report.

3.3 Test Setup

After installation of the gages, field-testing was performed on the fourth day. Testing was accomplished by using the following personnel: four traffic controllers, a data collector, a truck driver, and a radio operator. The radio operator communicated to the data collector when to start and stop the data acquisition system. Maintenance workers stationed at opposite ends of the bridge controlled the local traffic during each test run. The bridge was first closed to allow for calibration of the system. The truck driver was instructed to maintain proper speeds by the radio operator. Local traffic was stopped during data collection, but released after each truck passing.

3.4 Data Collection

Because the gages were spread over three different piers, the data had to be collected three times. The length of the data collection was different for each pier. A ten second pre-trigger was created to ensure recording of important data. Strain gages readings were taken at a frequency of 200 Hz.

18

A tandem-axle dump truck, as shown in Figure 3-4, was used to load the structure. The truck weight totaled 54 kips, with 17.2 kips on the front axle and 36.8 kips on the rear axles. For the pre-retrofit test, the vehicle had completed two passes at speeds of 0, 25, 45, and 65 mph for each direction of travel. Due to time limitations, the total number of passes for a single location was reduced. Two passes were completed at speeds of 0 and 65 mph for both directions. However, only one pass was made for 25 and 45 mph in each direction. This resulted with 36 loadings recorded for the strain gage data. Data was collected using a Waveform Data Acquisition and Analysis Module. It was connected to a laptop, which stored the data for later analysis.

3.5 Gage Protection

After testing had been completed, a protective coating was placed on the gages. The gages were left on the bridge for future testing. Figure 3-4 shows a prepared gage. Additionally, the wire was tied down to keep it from moving and damaging the connection to the gage.
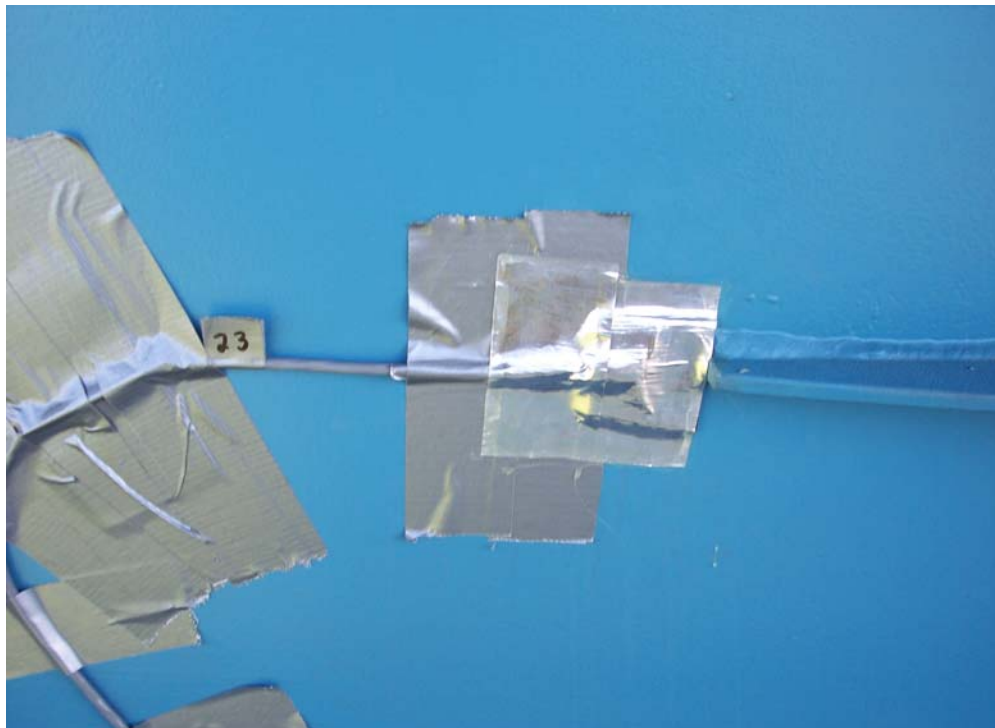
Figure 3-1: Snooper Used for Bridge Girder Access

Figure 3-2: Data Acquisition System

Figure 3-3: Loading Vehicle

Figure 3-4: Gage Protection

CHAPTER 4   BRIDGE BEHAVIOR GAGES

Results from the pre-retrofit gages were used to determine the degree of composite action between girders and the deck. In addition, the previous results provided information to improve the finite element model. Due to the fact that the focus of this report was to assess the effectiveness of the retrofit, only the comparison between the field measurements was analyzed.

4.1 Gage Locations

In the pre-retrofit test, gages 9-20 were used to gain information about the behavior of the bridge. In determining the effectiveness of the retrofit, the results of these gages were less important than the other gages. Therefore, three of the gages (13, 15, and 16) were moved from the bracing to new locations on the gusset plate. The remaining gages were placed at the same locations to provide continuity between the tests. Figure 4.1 shows the locations of the five gages in the web gap region. Figure 4.2 shows the locations of four gages in the gusset plate region.

4.2 Results

There was no retrofit implemented at the locations of these bridge behavior gages. Therefore, the stresses recorded by these gages were expected to be similar for the two tests. A comparison is presented in Table 4.1 and Table 4.2. Unfortunately, results from gage 10 could not be used in the analysis. The values recorded with gage 10 had a wide range and were non-uniform. The measurements from the other gages show that the stress values were relatively similar for both tests. This indicates that the retrofit had little impact on the stresses at these gage locations.
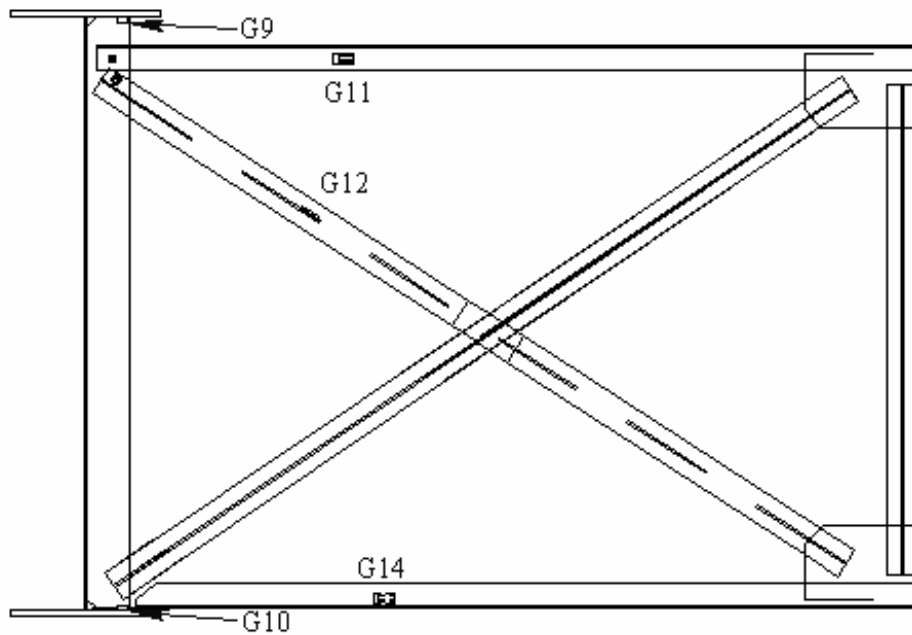
Figure 4-1: Web-Gap Region Gages

		Gage Number			
Eastbound		9	11	12	14
Positive Moment	Pre	-0.8	0.9	-0.5	-0.4
	Post	-0.4	1.2	-0.2	-0.3
Negative Moment	Pre	0.8	-0.4	0.6	0.6
	Post	0.3	-0.1	0.3	0.2

		Gage Number			
Westbound		9	11	12	14
Positive Moment	Pre	-0.6	1.1	0.7	-0.6
	Post	-0.1	2.1	0.8	-0.5
Negative Moment	Pre	0.7	-0.4	-0.4	0.5
	Post	0.6	-0.1	-0.1	0.3

Table 4-1: Average Stress (ksi) Comparison for the Web Gap Gages
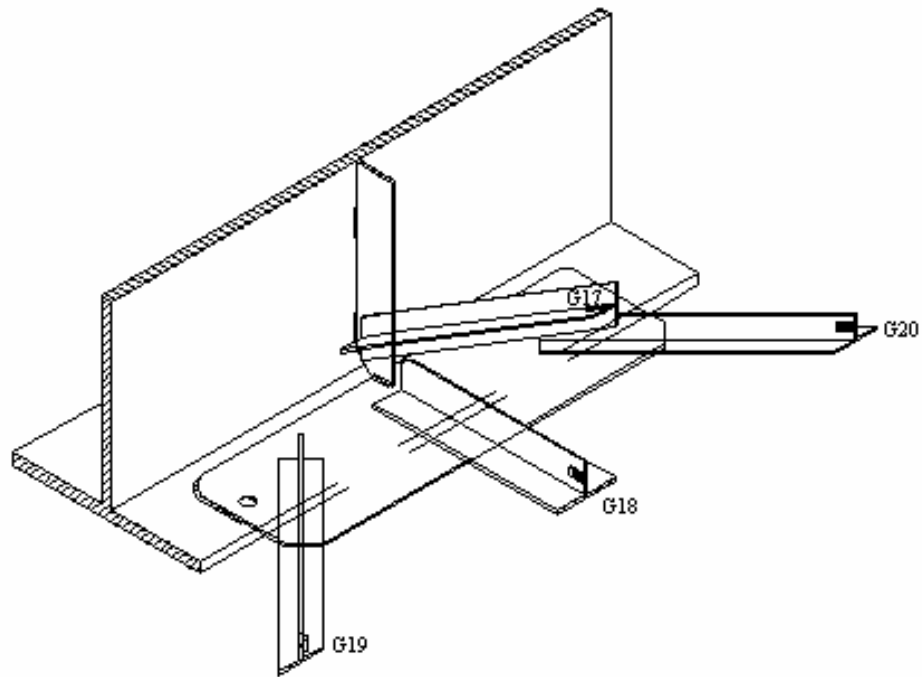
Figure 4-2: Gusset Plate Region Bracing Gages

		Gage Number			
Eastbound		17	18	19	20
Positive Moment	Pre	0.7	0.7	-0.9	1.4
	Post	0.8	0.8	-0.6	1.1
Negative Moment	Pre	-0.4	-0.4	0.6	-0.6
	Post	-0.1	-0.2	0.9	-0.4

Westbound		17	18	19	20
Positive Moment	Pre	-0.5	-0.5	1.1	-0.9
	Post	-0.3	-0.4	0.9	-0.6
Negative Moment	Pre	0.6	0.6	-0.7	0.6
	Post	0.5	0.6	-0.4	0.5

Table 4-2: Average Stress (ksi) for Gusset Plate Bracing Gages

CHAPTER 5   WEB-GAP CRACKING

In this chapter, the retrofit of the web-gap region is described. The repair strategy and gage locations are presented. In addition, stresses from both field investigations are compared.

5.1 Repair Strategy

The web-gap region had been previously repaired in 1986, as described in Chapter 2. Because that repair was ineffective, a different retrofit scheme was implemented to fix the connection. Part of the strategy was to create a positive connection between the upper flange and the connection stiffener. To achieve this connection, two brackets were added and were connected to the upper flange by two welded studs. The brackets were then bolted to the connection stiffener. In addition, stop holes were drilled in the web to arrest the horizontal cracking. To repair the lower web-gap region, the stiffener was fillet welded to the gusset plate.

5.2   Gage Locations

It was not necessary to change the location of any of the gages from the previous field investigation in the web gap region. Therefore, eight gages were placed on diaphragm F2 to measure stresses. Figure 5-1 shows the locations of the four gages in the upper web-gap region. Two gages were placed on the interior side and exterior side of the web. Due to space limitations, the gages could not be placed at the exact location of the horizontal cracks. Therefore, the gages were placed in line with each other. This alignment allowed the stress in the gages to be extrapolated to the crack location. Figure 5-2 shows the other four gages in the lower web gap region. These four gages were placed in a similar formation as the upper web-gap gages.

5.3 Results

The post-retrofit measurements had similar patterns to those observed in the pre-retrofit measurements. Once again, the stress values for the upper web-gap region were higher in the westbound direction. In addition, gages closer to the flange recorded higher stress values. The average stress values for both pre-retrofit and post-retrofit are shown in Tables 5-1 and 5-2. A comparison of the extrapolated values is presented in Table 5-3.

According to the results, the retrofit procedure succeeded in reducing the stresses in the web-gap regions. Using absolute stress values, reductions of up to 90 percent were observed for some gage locations. These reductions are consistent with the finite element model created by Dr. Zhao (Zhao and Roddis, 2003). Smaller pre-retrofit absolute stress values generally showed a smaller percent reduction in stress values.

For the upper web-gap extrapolated values with the truck moving westbound, the average maximum stress was reduced from 35.4 ksi to 9.3 ksi. For the truck moving eastbound, the maximum average stress value changed from 12.6 ksi to 6.7 ksi. These values show a significant decrease in stress at the critical point where a crack might form in the upper web gap region. In the lower web gap region, the absolute value of the stress was reduced, but the margin was not as pronounced as in the upper web-gap region.
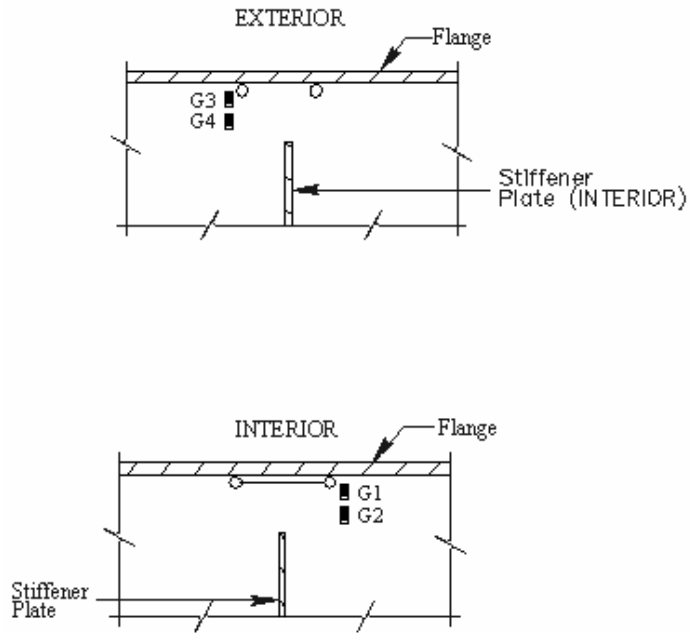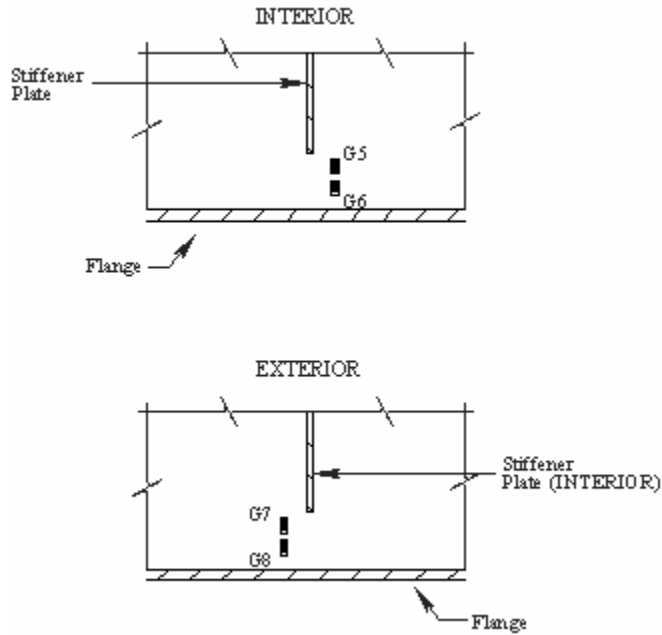
Figure 5-1: Upper Web Gap Gages

		Gage Number			
Eastbound		1	2	3	4
Positive Moment	Pre	-9.1	-4.5	9.7	5.1
	Post	-2.1	-0.4	5.0	2.7
Negative Moment	Pre	2.6	0.9	-2.3	-0.7
	Post	0.3	0.2	-0.3	-0.2

Westbound		1	2	3	4
Positive Moment	Pre	-24.7	-9.3	25.3	9.2
	Post	-4.5	-1.1	7.0	3.3
Negative Moment	Pre	1.7	0.6	-1.6	-0.8
	Post	0.2	0.2	-0.3	-0.2

Table 5-1: Average Stress (ksi) Comparison for the Upper Web Gap Gages

Figure 5-2: Lower Web Gap Gages

		Gage Number			
Eastbound		5	6	7	8
Positive Moment	Pre	1.2	-1.2	-2.5	-0.5
	Post	0.3	-0.4	-0.6	-0.6
Negative Moment	Pre	-0.4	0.6	0.9	0.9
	Post	-0.4	0.3	0.3	0.3

Westbound		5	6	7	8
Positive Moment	Pre	-0.7	1.7	0.9	-2.0
	Post	-0.6	0.3	0.3	-1.0
Negative Moment	Pre	0.7	-0.6	-0.6	1.0
	Post	0.3	-0.3	-0.4	0.4

Table 5-2: Average Stresses (ksi) Comparison for the Lower Web Gap Gages

		Gage Number			
Eastbound		1 & 2	3 & 4	5 & 6	7 & 8
Positive Moment	Pre	-11.9	12.6	-2.4	1.8
	Post	-3.0	6.7	-0.7	-0.6
Negative Moment	Pre	3.6	-3.2	1.2	1.0
	Post	0.3	-0.4	0.6	0.4

Westbound		1 & 2	3 & 4	5 & 6	7 & 8
Positive Moment	Pre	-34.4	35.4	3.0	-5.7
	Post	-6.6	9.3	0.7	-2.7
Negative Moment	Pre	2.4	-2.1	-1.3	2.9
	Post	0.3	-0.3	-0.6	1.5

Table 5-3: Average Stresses (ksi) Comparison for Extrapolated Values

CHAPTER 6   GUSSET PLATE CRACKING

Work completed in the gusset plate region is presented in this chapter. The repairs completed are discussed. The reason for moving gages is given along with a comparison of the test results. In addition, the position and results of new gage locations are explained.

6.1 Repair Strategy

Some gusset plates were repaired in 1986 due to the presence of fatigue cracks. The only plates that were repaired were located nearest to the piers. The repair consisted of bolting a larger gusset plate to the flange and removing all welds in the connection (Figure 6-1). This repair strategy was effective but was not done for every gusset plate.

After 1986, cracks developed at diaphragms next to repaired plates. To repair these gusset plates, KDOT used a slightly different strategy. Figure 6-2 shows the new retrofit scheme that was used. All cracked welds were repaired and the gusset plates were bolted to the lower flange. In addition, some gusset plates were replaced due to damage.

6.2 Gage Locations

Several changes were made to the pre-retrofit gage locations. First, the gusset plate at Pier 29 had been replaced due to damage. The replacement gusset plate was not identical to the pre-retrofit plate. Because the purpose of the measurements was to compare the behavior of a gusset plate that had been repaired, it was necessary to use a gusset plate that had an identical geometry to the original plate. Therefore, the decision was made to move the gages to the gusset at Pier 28 because that gusset plate had not been replaced. Second, three gages that were not in the pre-retrofit test were moved to the gusset plate region. It was difficult to determine the exact source of the cracking from the pre-test data. To help determine the source of cracking, these three

gages were placed on the gusset plate perpendicular to the girder. In addition, two gages were placed at the same location on the top and bottom of the gusset plate to investigate whether bending was occurring in the plate. A strain gage rosette was placed in the same location as was done in the pre-retrofit test. Placement of the gages can be seen in Figure 6-3 and Figure 6-4.

6.3 Results

A comparison of the rosette gage values is presented in Table 6-1. The data indicates little difference between pre-retrofit and post-retrofit measurements. This was expected because, from the perspective of the gage location, the connection was largely unchanged. However, the two tests were performed at different pier locations. Because the two test results appear to be relatively the same, the decision to use the same type of gusset plate was justified by the similar results. In addition, this indicates that conclusions drawn from the pre-retrofit measurements apply to the post-retrofit analysis.

Information from the pre-retrofit measurements was not sufficient to determine the origin of the cracks that formed on the gusset plate. There were a few hypotheses, but it was not possible to derive a definitive conclusion based on the information gathered. Three gages were relocated to the gusset plate region to provide more data. Average stresses in these gages can be seen in Table 6-2. In addition, the variation of stress with time for the gages 13, 15, and 16 is presented in Appendix D. In particular, the relationship between these gages is of interest because of their location relative to one another. One hypothesis presented in the first field report (Marshall et al., 2005) was that cracking was caused by lateral distortion of the brace. This distortion would induce a prying action in the gusset plate. According to the graphs in Appendix D, the data supports the theory that the gusset plate experienced bending during loading. While this does not prove that this was the only cause of the cracking, it does show that prying action contributed.
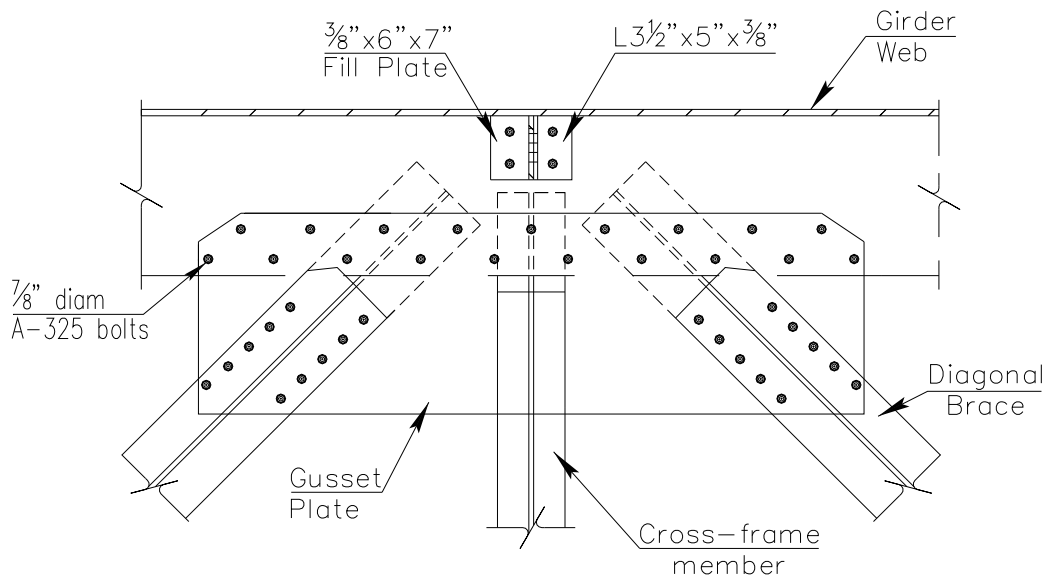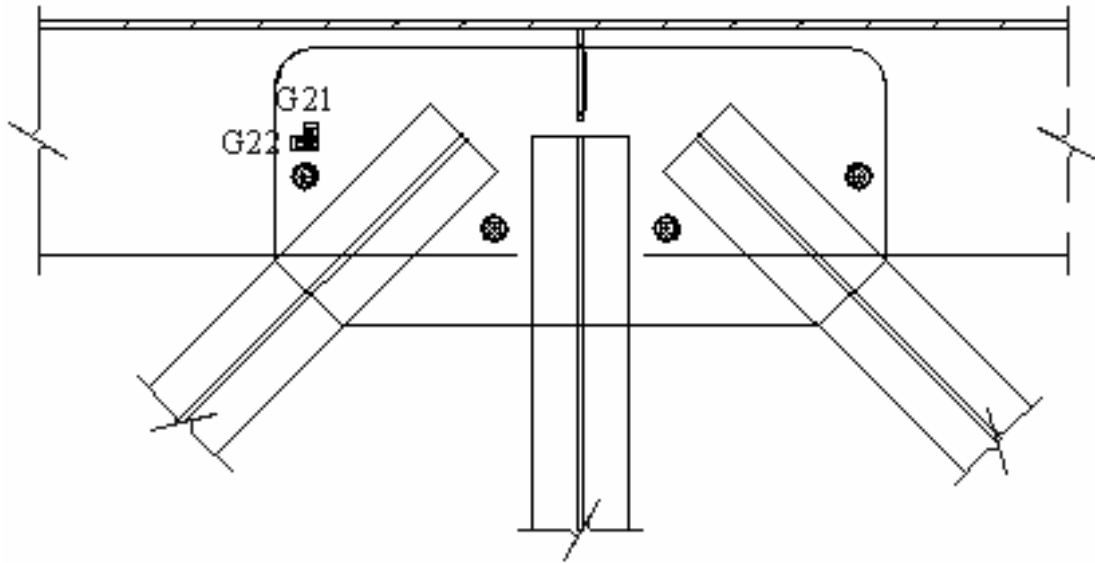
Figure 6-1: 1986 Repair of Gusset Plate (Only Gusset Plates Closest to Piers)
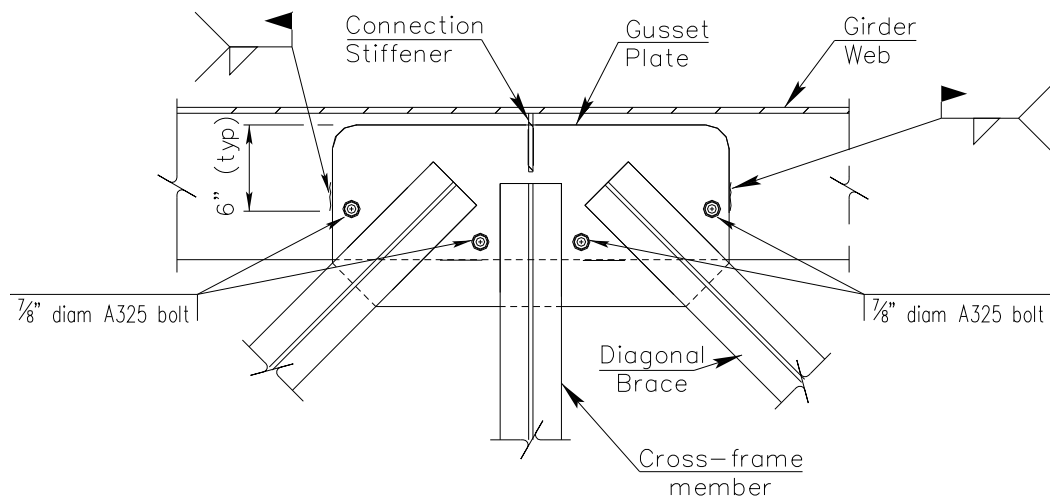
**Figure 6-2: Repaired Gusset Plate (Remaining Gusset Plates)**

Figure 6-3: Location of the Rosette Gage

		Gage Number	
Eastbound		21	22
Positive Moment	Pre	-0.5	1.1
	Post	-0.1	1.0
Negative Moment	Pre	0.6	-0.7
	Post	0.7	-0.6

Westbound		21	22
Positive Moment	Pre	0.5	0.5
	Post	0.5	0.5
Negative Moment	Pre	-0.4	-0.5
	Post	-0.1	-0.4

Table 6-1: Comparison of Average Stress Values (ksi) in Rosette Gage

G15 (Top), G13 (Bottom)   G16 (Top)
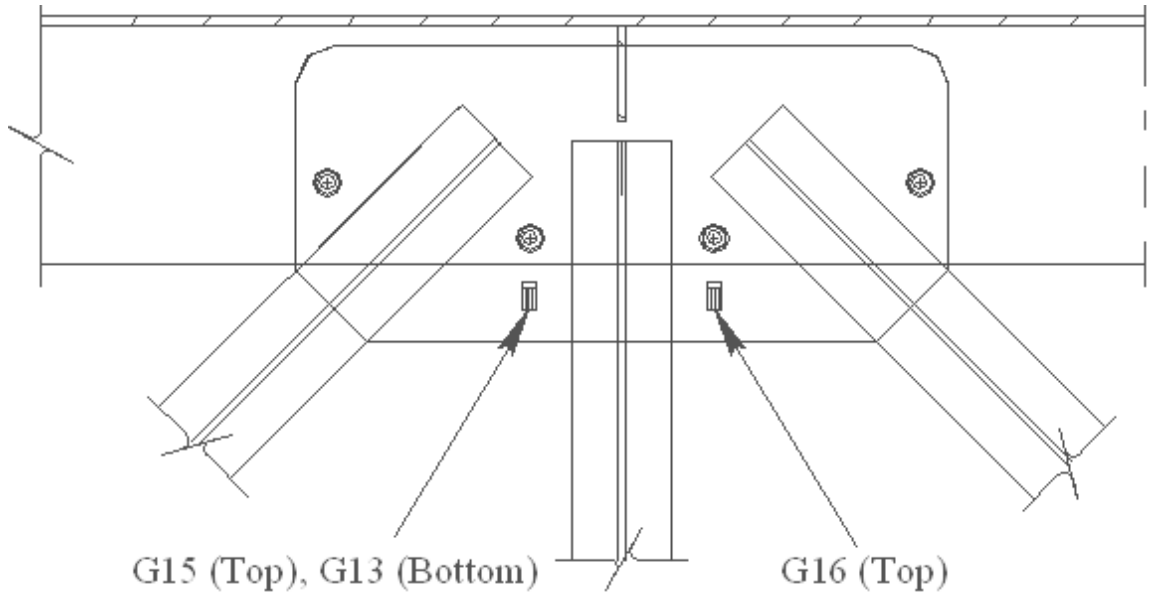
Figure 6-4: Location of Relocated Gages

		Gage Number		
Eastbound		13	15	16
Positive Moment	Post	1.1	-0.3	-0.2
Negative Moment	Post	-0.1	1.2	0.7

Westbound		13	15	16
Positive Moment	Post	-0.1	0.8	0.5
Negative Moment	Post	0.7	-0.5	-0.2

Table 6-2: Average Stress Values (ksi) for Relocated Gages (Post Retrofit Only)

CHAPTER 7   LONGITUDINAL STIFFENER CRACKING

This chapter discusses a comparison of pre-retrofit and post-retrofit test results. Repairs for the longitudinal stiffener are discussed. In addition, the gage location is shown along with the results of the test.

7.1 Repair Strategy

Two repairs were performed on the longitudinal stiffener. First, cracks in the butt welds of the stiffener were repaired. This was accomplished by grinding off the butt welds and re-welding them. Second, the end of the longitudinal stiffener was tapered to reduce the stress concentration because the termination point of the stiffener is classified as a category E detail according to the 2004 AASHTO LRFD specifications. This repair was used as a preventative measure, and the second repair is shown in Figure 7-1.

7.2 Gage Location

As in the pre-retrofit test, only the effect of the tapering repair was investigated. A single gage was placed at the same location as in the pre-retrofit test. The gage was located closest to Span 29. The placement is shown in Figure 7-2.

7.3 Results

Comparison of the data can be found in Table 7.1. According to the data, there was a slight decrease in average stress at the gage location. The data obtained was not sufficient to determine the effectiveness of the repair. Additionally, a study of the stiffener region was conducted by Santiago Bonetti at the University of Kansas. The report is included as Appendix F.
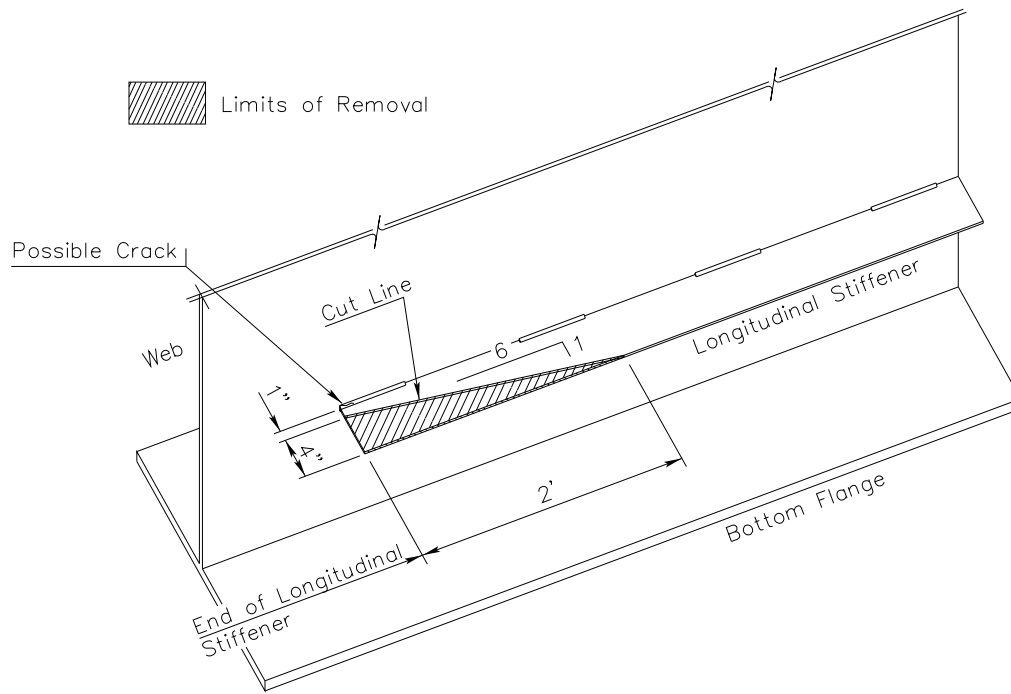
Figure 7-1: Completed Longitudinal Stiffener Repair
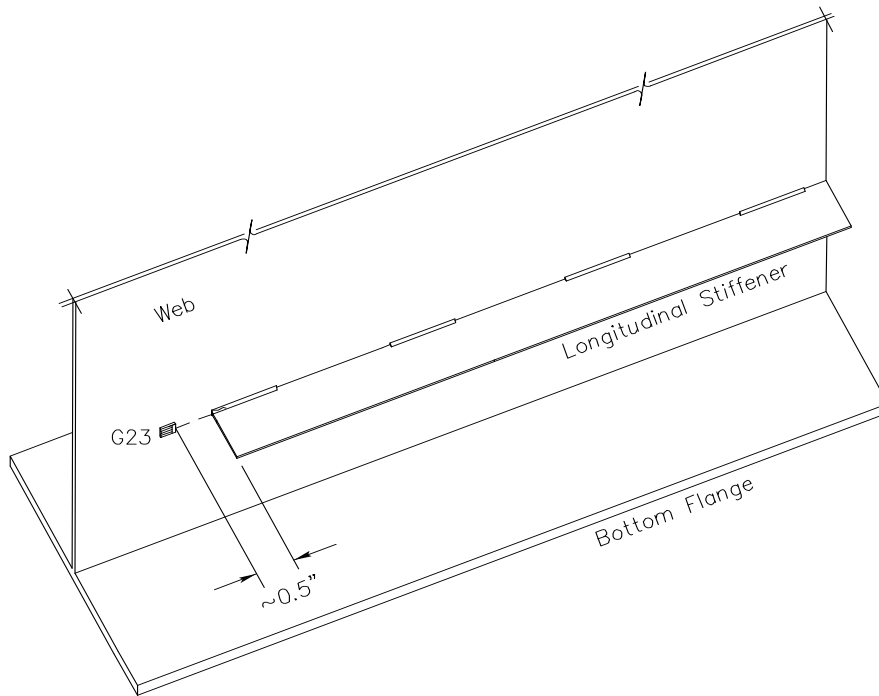
Figure 7-2: Longitudinal Stiffener Gage Location

		Gage Number
Eastbound		23
Positive Moment	Pre	4.6
	Post	3.1
Negative Moment	Pre	-1.8
	Post	-1.0

Westbound		23
Positive Moment	Pre	3.4
	Post	2.6
Negative Moment	Pre	-1.8
	Post	-1.1

Table 7.1: Average Stress (ksi) Comparison for Longitudinal Stiffener

CHAPTER 8   CONCLUSIONS

Throughout the post-retrofit field measurements and report, continuity with the pre-retrofit test was maintained whenever possible to provide accurate comparisons between the two conditions. The comparison between the two sets of measurements resulted in the following conclusions.

1. Stresses in the upper web gap region were reduced dramatically by the retrofit. This is expected to increase the fatigue life of the connection. The results were in agreement with the model created by Dr. Zhao.
2. Stresses in the lower web gap region were decreased, but in a smaller amount. Stresses in this region are not expected to produce fatigue cracking.
3. Stresses in the gusset plate did not change drastically, but information from new gage locations suggest that prying action was involved in forming the fatigue cracks.
4. Stress was slightly reduced at the termination of the longitudinal stiffener, but the overall benefit of the retrofit is not well defined.
5. The overall post retrofit experimental analysis of the Tuttle Creek Bridge supports the proposed analytical changes recommended by Dr. Zhao.

REFERENCES

AASHTO LRFD, 2004

LRFD Bridge Design Specifications, 3rd Edition. LRFDUS-3 or LRFDSI- 3, American Association of State Highway and Transportation Officials, Washington, D.C.

AASHTO, 2002.

Standard Specifications for Highway Bridges, 17th Edition, HB-17, American Association of State Highway and Transportation Officials, Washington, DC.

Fisher et al., 2001

John W. Fisher, Efim Statnikov, and Lionel Tehini. "Fatigue Strength Enhancement by Means of Weld Design Change and the Application of Ultrasonic Impact Treatment". ATLSS Engineering Research Center, Lehigh University, Bethlehem, Pennsylvania.

IOtech, Inc., 1997

IOtech, Inc. Wave Book User's Manual, Cleveland, Ohio.

Marshall et al., 2005

Nathan Marshall, G. Ramirez, W.M. K. Roddis, S. T. Rolfe, A. B. Matamoros. "Field Instrumentation and Analysis of the Tuttle Creek Bridge Br. No. 16-80-2.24," Report No. KTRAN: KU-04-5, Kansas Department of Transportation, Topeka, Kansas.

Vishay Micro Measurements, Inc., 2000

Vishay Micro Measurements Group, Inc. (2000). Products and Technical Binder, Raleigh, North Carolina.

Wright, 1996

   William Wright. Post-Weld Treatment of a Welded Bridge Girder by Ultrasonic Impact Treatment. Federal Highway Administration, Turner-Fairbank Highway Research Center, McLean, Virginia.

Zhao and Roddis, 2003

   Yuan Zhao and W. M. Kim Roddis. "Fatigue Prone Steel Bridge Details: Investigation and Recommended Repairs", Report No. KTRAN: KU-99-2, Kansas Department of Transportation, Topeka, Kansas.

APPENDIX A ULTRASONIC IMPACT TREATMENT

A.1 Overview

Ultrasonic impact treatment (UIT) was developed in 1972 by Dr. Efim Statnikov for use in Soviet Union naval ships. UIT induces compressive stresses into a welded joint, which increases fatigue initiation life. To accomplish this, UIT equipment impacts the material with a very high frequency (27 kHz) to create a plastic deformation in the material. It was introduced to the Federal Highway Administration in a demonstration at the Turner-Fairbank Research Center on June 6, 1996. Since then, limited research has been conducted in the United States to examine the benefits of UIT. This research has shown that UIT can increase the fatigue initiation life of welds in new and existing bridges.

A.2 Method of Application

UIT is performed with a handheld tool, electronic control box, and water cooling system. The handheld tool weighs approximately eight pounds and is much easier to control than other weld treatment systems such as shot peening due to the fact that the UIT process occurs at a very high frequency. In addition, the high frequency range makes the process relatively quiet compared to other systems. The metal is treated by placing the tip of the handheld tool at a 45-degree angle to the surface being treated. The tool is then moved back and forth over the area being treated. This creates a small depression in the weld, resulting in compressive stresses. Visual checks can be made to determine if the area has been properly treated.

A.3 Research

Since UIT is a relatively new procedure, additional research is needed to determine the range of applications that would benefit from the treatment. Research was conducted by the FHWA to determine the effectiveness of the treatment. After this initial research, the FHWA funded further testing conducted at Lehigh

University. The research conducted at Lehigh University was performed by Dr. John Fisher. This research is summarized in the following sections.

A.4 Wright (1996)

Wright, at the FHWA research center, performed an analysis of the UIT as it was applied to fillet welds in a typical bridge girder. The purpose of this study was to determine if UIT had any effect on the fatigue life of fillet welds.

Eight mm fillet welds were placed on both sides of a girder web using the submerged arc welding (SAW) process to connect a transverse stiffener to the web, a category C detail. Testing consisted of first saw cutting six cruciform-type fatigue specimens. Weld toes were treated with UIT. To complete the process, numerous passes were made over the weld toes. The number of passes and speed of the application were not recorded for the test procedure.

Specimens were load tested in a sinusoidal pattern at a frequency of 20 Hz. The stress range applied was around 130 MPa (18.9 ksi) with an R-ratio (min load/max load) of .5. The load cycle was applied until fatigue cracks developed and the specimen completely failed.

The results indicated an improvement in the fatigue life of the ultrasonic impact treated welds. According to the results, welds that had been treated showed a fatigue life over eight times greater than the welds which had not been treated.

A.5 Fisher et al (2001)

Fisher et al (2001) performed further analysis of UIT. The purpose of the study was to determine the overall benefits gained from using UIT, which included examining both structural benefits (increased fatigue life of the weld) and application benefits (less difficulty, reduced implementation time, and reduced costs). Eighteen specimens were tested. The specimens were 18 ft long, 27 in. deep, W27x129 rolled wide-flange beam sections with 1.1 in. thick flanges. The web of the girder was 0.61 in. thick. The transverse stiffeners were 0.5 in. thick. All specimens were fabricated

according to AWS specifications. The transverse stiffeners were provided over the full depth of the girder and were welded at the top and bottom flange and on the web. Cover plates were provided on both ends of the girder. For seven of the specimens, one cover plate was welded on all sides to the flange with a 0.5 in. fillet weld. For two of the specimens, the second cover plate did not have any end welds. For the remaining specimens, both cover plates had 1 in. fillet end welds. To reduce stress concentrations between the 1 in. end weld and the 0.5 in weld, a smooth transition betweeen the welds was made.

Two critical areas were defined. The welds at the junction of the transverse stiffener and the bottom flange were defined as critical, as was the lower portion of the junction between the stiffener and the web. These were category C details. All end welds on the cover plate were considered to be critical, and were category E details. All critical details were treated by the UIT procedure. Three passes were used to create a smooth transition between the weld toe and the material.

Tests were conducted at a constant amplitude fatigue loading. The beams were visually inspected with use of a magnifying glass. Tests were continued until a fatigue crack formed in the critical details of the specimens. If a crack formed in the web first, the test was stopped, and a hole was drilled to stop the crack.

According to data gained from the test, the use of UIT is very beneficial to the fatigue life of the critical details. For the cover plate, the fatigue life improved from that of a category E detail to the life of a category C detail. For the stiffener, the detail improved from a category C performance to a category B detail performance level.

The study also analyzed four bridges that were experiencing fatigue cracking. The bridges were located on Interstate 66 and were all built in 1979. The bridges were experiencing fatigue cracking at the top of the connection plates where the plates were not positively connected to the flange. It was determined that a retrofit would fix this problem. It was also decided to retrofit the bottom of the connection plates before fatigue cracking initiated at that location.

For purposes of this study, two alternatives were considered: a conventional retrofit and ultrasonic impact treatment. The study concluded that the latter was considerably more efficient. To complete the UIT retrofit, the connection plates just needed to be welded to the flange and then treated. According to the study, this would take much less time than a conventional retrofit. Since the bridges were in use, being able to complete the repairs in a small time frame was important. In addition, the cost of the UIT alternative was less than the cost for the conventional retrofit. Due to these factors, UIT was the more attractive of the two choices.

A.6 Summary

The benefits from UIT appear to be large, but very few details have been currently tested. Thus, it would seem that fatigue tests should be conducted using details that represent possible KDOT applications. Therefore, specimens that exhibit details used in current KDOT structures should be fabricated and fatigue tested. This testing would provide specific UIT information for KDOT structures.

APPENDIX B   PREVIOUS KU RESEARCH

B.1 Overview

Initial research on the Tuttle Creek Bridge was completed by Yuan Zhao, a former University of Kansas Ph. D. student. The focus of her report (*Fatigue Prone Steel Bridge Details: Investigation and Recommended Repairs*) was to analyze distortion induced cracking of steel bridge structures. The Tuttle Creek Bridge was one of five bridges analyzed in her report. The analysis of the stresses in the structure was completed using a finite element model created using ANSYS. After the causes of cracking were investigated, multiple retrofit strategies were compared to determine the most effective repair.

B.2 Finite Element Models

A coarse model was made to analyze a typical intermediate span of the bridge. An HS15 truck with 10% wheel load was used to load the structure. In the analysis, the deck was assumed to act non-compositely. In addition, the truck loading was only placed in the westbound lane under the assumption that the bridge would act symmetrically.

Sub-models were created to analyze the upper and lower web-gap regions. Each repair strategy had a separate sub-model which used the forces found in the coarse model to predict the stresses in the connection. These stresses were then compared to determine the most effective retrofit.

B.3 Retrofit Strategies

Four retrofit strategies were analyzed in the report: cutting a 4.5" slot into the stiffener, cutting a 12.5" slot into the stiffener, permitting the first intermittent welds to break, and positively connecting the stiffener to the flanges.   The analysis concluded that positively connecting the stiffener to the flange would be the most effective retrofit.   The analysis predicted that the stresses would be reduced by

approximately 90% of their original value. The results from the post-retrofit analysis supported this conclusion as discussed in Chapter 5.

APPENDIX C INSTRUMENTATION PROCEDURE

C.1 Gage Installation

Gage installation was the majority of the work completed in the field testing. Placement of the gages was performed using a snooper to reach underneath the bridge. Two installers were able to work in the bucket along with the operator. Materials for installation were prepared before application of the gages.

C.1.1 Gages

Twenty-six single element gages were used in this test. Additionally, one 90° rosette was used. The single element gages were purchased from Micro Measurements, Inc. The part number for these gages was CEA-06-250UW-350. The part number for the 90° rosette was CEA-06-250WQ-350. It was also purchased from Micro Measurements, Inc. The resistance of the gages was 350±0.3% ohms.

C.1.2 Grinding

The first step in installation was removal of the paint from the gage area. This task was accomplished by using a braided wire wheel mounted on a grinder. A generator on the snooper powered all electrical equipment. Paint, rust, and grime were easily removed with the heavy-duty wire wheel. Grinding continued until the base metal was clearly visible. A patch approximately four inches long by three inches wide was created for each gage location. The ground surface appeared gray and dull. Grinding was performed for all locations prior to further surface preparation since grinding could easily contaminate other gage locations. Dust masks and eye protection were used since the paint was lead-based. After removing the paint, each gage location was labeled on the bridge using a permanent marker.

C.1.3 Surface Preparation

After the paint had been removed, additional surface preparation was needed. First, the location was sprayed with degreaser and wiped clean. Next, M-Prep Conditioner A was sprayed on the location. Then, 320-grit sandpaper was used to clean the surface. The sandpaper was kept moist with the conditioner while being used. After using the sandpaper, the surface was wiped using gauze pads until no discoloration was seen on the pads. The M-Prep Conditioner A was then applied again and the procedure repeated for 400-grit sandpaper. After the two applications of the conditioner, M-Prep Neutralizer was applied to the area. The same procedure for both 320-grit and 400-grit sandpaper was repeated using the neutralizer. The gage placement was then drawn outside the conditioned area with a permanent marker.

C.1.4 Gage Placement

Before going into the field, the gages had been taped down to a plastic board to keep them from being scattered during the installation. Care was taken to ensure that the edges of the tape and the edges of the gages were parallel to one another. After the surface was prepared, the gages were taped to the surface in their proper positions. Then, the tape was slowly folded back to reveal the gage surface. The tape was folded at a low angle compared to the surface to prevent bending of the gage. Next, M-Bond 200 catalyst was brushed onto the gage surface. After allowing the catalyst to dry for one minute, a small drop M-Bond 200 adhesive was placed at the fold of the tape. The adhesive was spread by gently lowering the gage back down to the surface. Firm pressure was applied to the gage for one minute to allow the adhesive to bond.

C.1.5 Soldering

After the gage had been adhered to the location, it was allowed to dry. Once the adhesive had dried, the cellophane tape was removed from the gage. The tape was peeled directly back to prevent any upward force on the gage. To prepare for soldering, drafting tape was placed next to the soldering tabs. Then, soldering flux

was applied to the two tabs. The shielded part of the wire was duct taped to the bridge to hold the wire in place. Next, the soldering iron was cleaned on a damp sponge. A small amount of solder was then put on the iron. The exposed wire was positioned on the tab and soldered. The two wires were then checked with an ohm meter to make sure a proper connection was established. M-Coat A Polyurethane was applied to both the strain gage surface and the exposed wires to protect against moisture. M-Coat B was brushed over area after the M-Coat A had dried.

C.2 Wire Preparation

To connect the gages to the data acquisition system, shielded wiring from Newark InOne was purchased. Belden Electronics specified the wire as 326DFV. The shielding prevented any damage from occurring due to setting up the wire.

The wire was prepared in the lab before going to the test site. The wire was cut and bundled in the lab. On one end of the wire, spade terminals were connected. This was completed removing about 2" of shielding and stripping 0.5" from the three strands. Then, the red strand was connected to one spade terminal, while the black and white strands were connected to the other spade terminal.

On the other end of the wire, 2" of shielding were removed from the wires. The three wire strands were then stripped 1.5" from the ends. To prepare the red strand, one wire from the braid was left straight while the rest were wrapped around that wire. For the black and white strands, one wire from one braid was left straight. Then, the braided wire for both strands was wrapped around the exposed base of the one wire. Both wrappings were covered by electrical tape. The tape covered approximately 0.5" of the exposed 1.5". Duct tape was then wrapped around the electrical tape to help hold and protect the strands.

C.3 Data Acquisition System

An IOtech Waveform Data Acquisition and Analysis Module were used as the data acquisition system during the tests. A laptop computer was connected to the

Wavebook to store the data. The Wavebook, specified as a WB516, interchanged with three WBK16/SSH modules. Software for the Wavebook was installed on the laptop computer that was used. Terminal strips were used to connect the modules to the wiring. The terminal strips were configured in a quarter-bridge setting. These strips were mounted on a plywood sheet. The spade terminals from the wires screwed into the strips. Cables connected the strips to the three modules. Each terminal strip was labeled.

For gages near Spans 29 and 28, the data acquisition system was placed on the closest pier. For the other gages, the data acquisition system was placed on the shoulder of the roadway. The wires were placed along the bridge and secured with zip ties to prevent movement.

Prior to testing, all equipment was tested for accuracy and precision. After placing the gages and wires, the data acquisition system was tested at each location to check the connections.

APPENDIX D STRAIN GAGE DATA

The exact cause of cracking in the gusset plate was unknown after the first field investigation. In order to help determine why the cracking was occurring, three gages were moved to new locations on the gusset plate. Gage 13 was placed on the bottom side of the gusset plate with gage 15 placed directly above it on the top side. Gage 16 was placed in a similar location as gage 15 on the opposite side of the center brace. The locations are shown in Figure 6-4.

The stress over time for these gages is shown in Figures D-1 through D-11. The majority of the data supports the theory that there is bending force acting on the gusset plate during loading. This is illustrated when gage 13 experiences a stress that is opposite of the stress in gage 15. Gage 16 is also provided as a reference but is not directly related to the position of gage 13. Due to the majority of the tests exhibiting this relationship, prying action is occurring in the plate and is contributing to the formation of cracks.
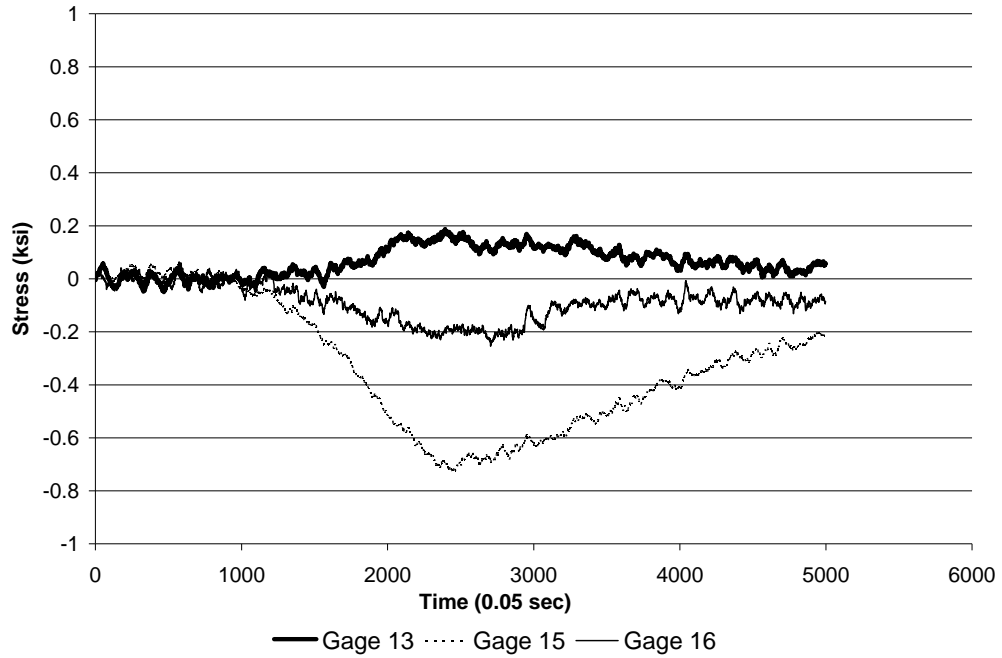
Figure D-1: Strain Gage Results Due to Truck Loading Westbound 5 mph A
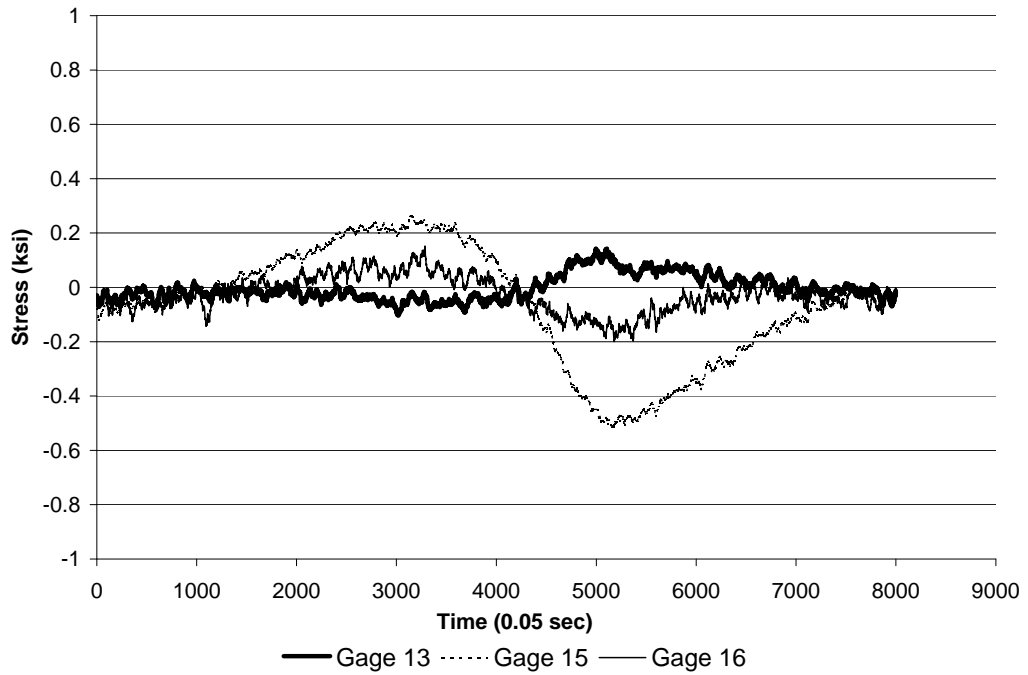
Figure D-2: Strain Gage Results Due to Truck Loading Westbound 5 mph B
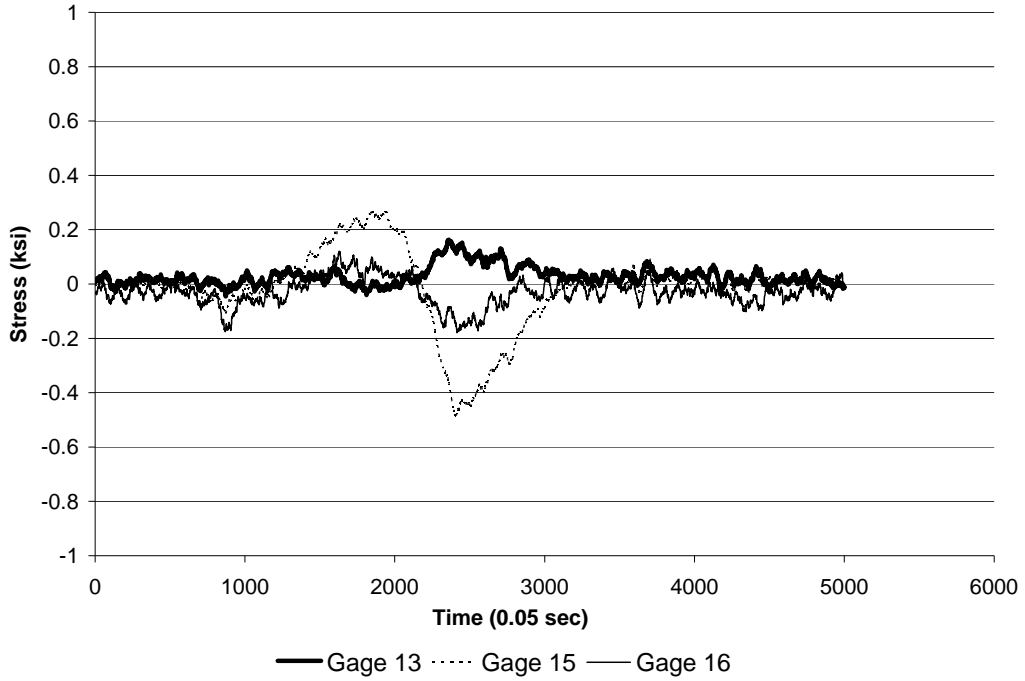
Figure D-3: Strain Gage Results Due to Truck Loading Westbound 25 mph
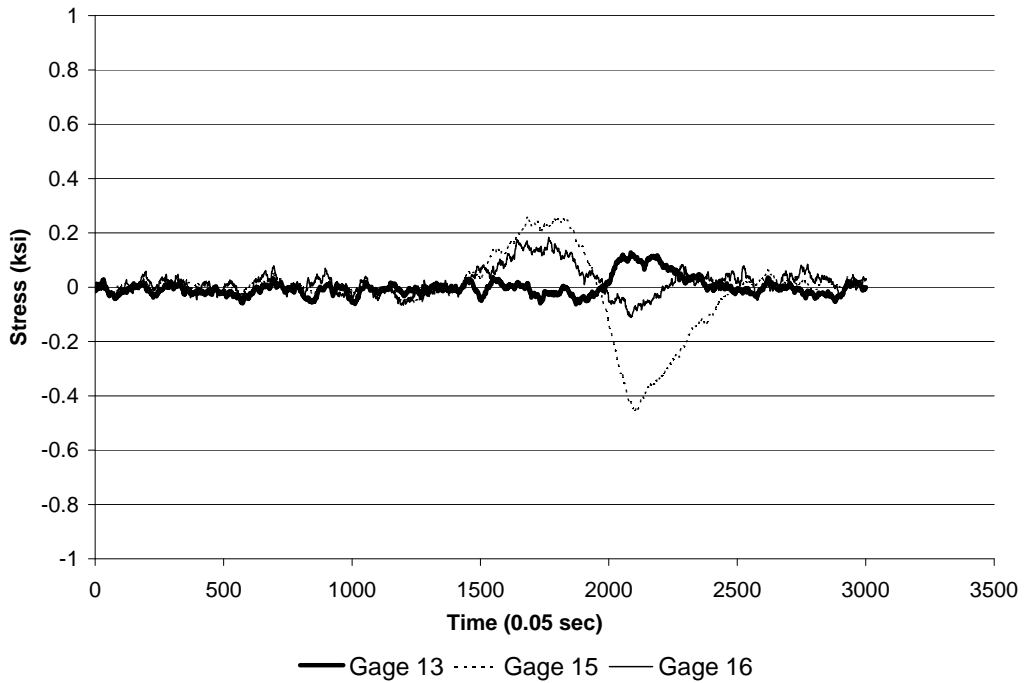
Figure D-4: Strain Gage Results Due to Truck Loading Westbound 45 mph
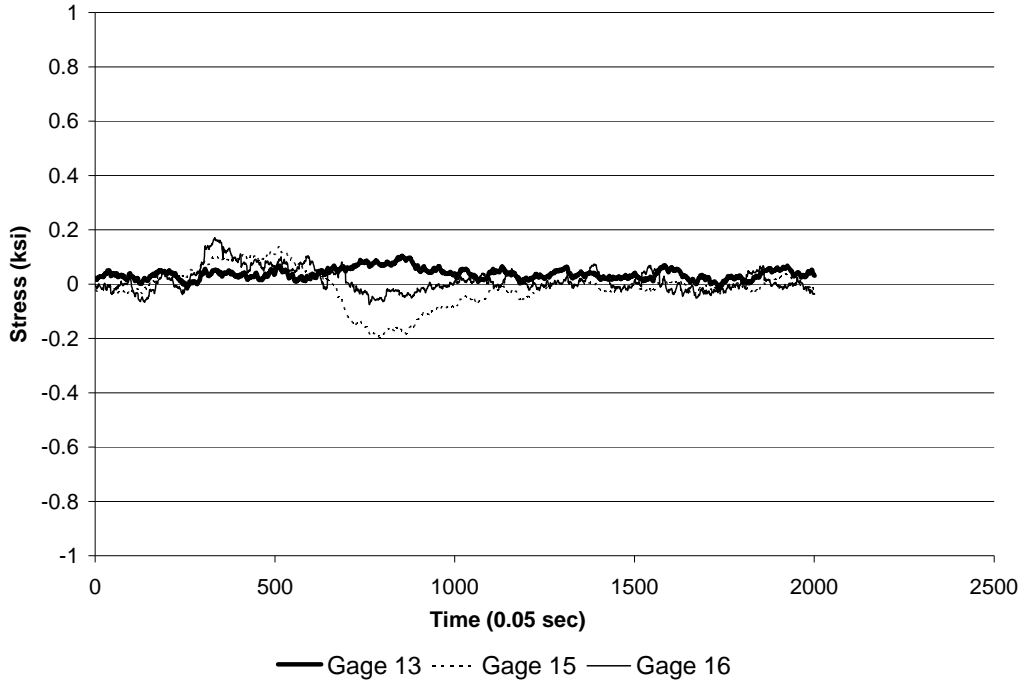
Figure D-5: Strain Gage Results Due to Truck Loading Westbound 65 mph A
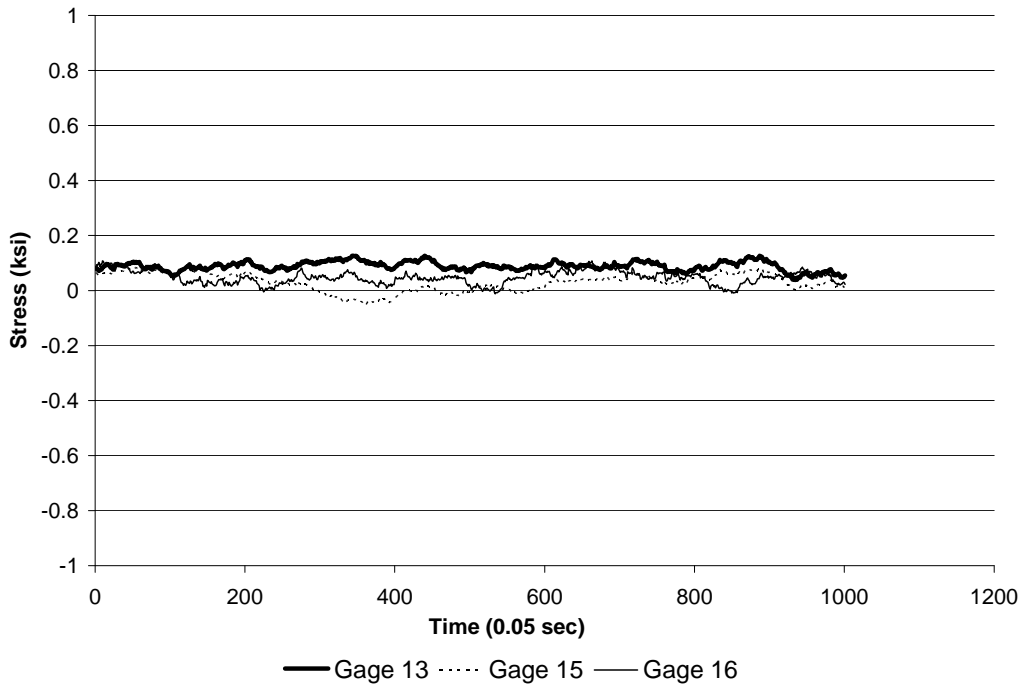
Figure D-6: Strain Gage Results Due to Truck Loading Westbound 65 mph B

54
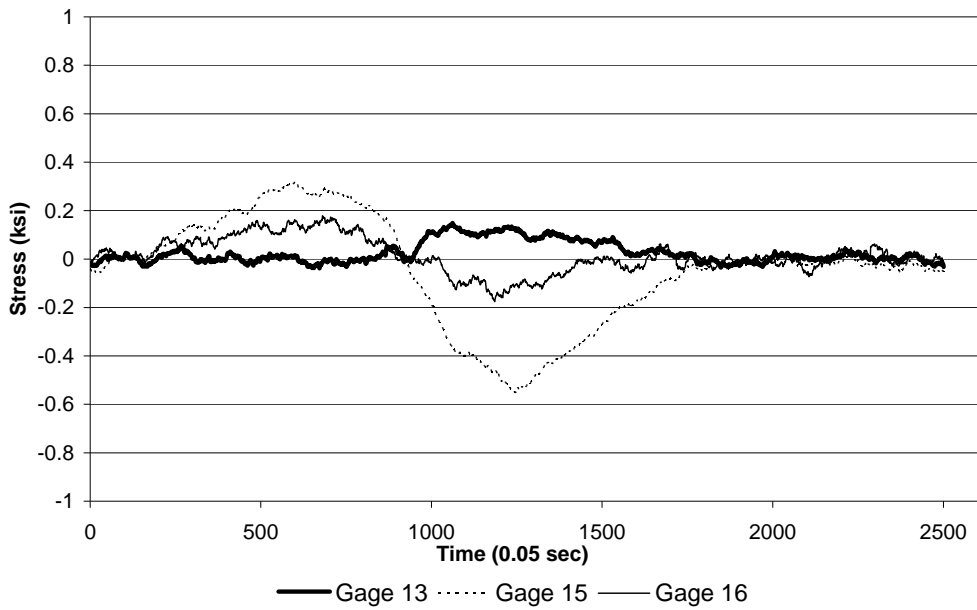
Figure D-7: Strain Gage Results Due to Truck Loading Eastbound 5 mph A
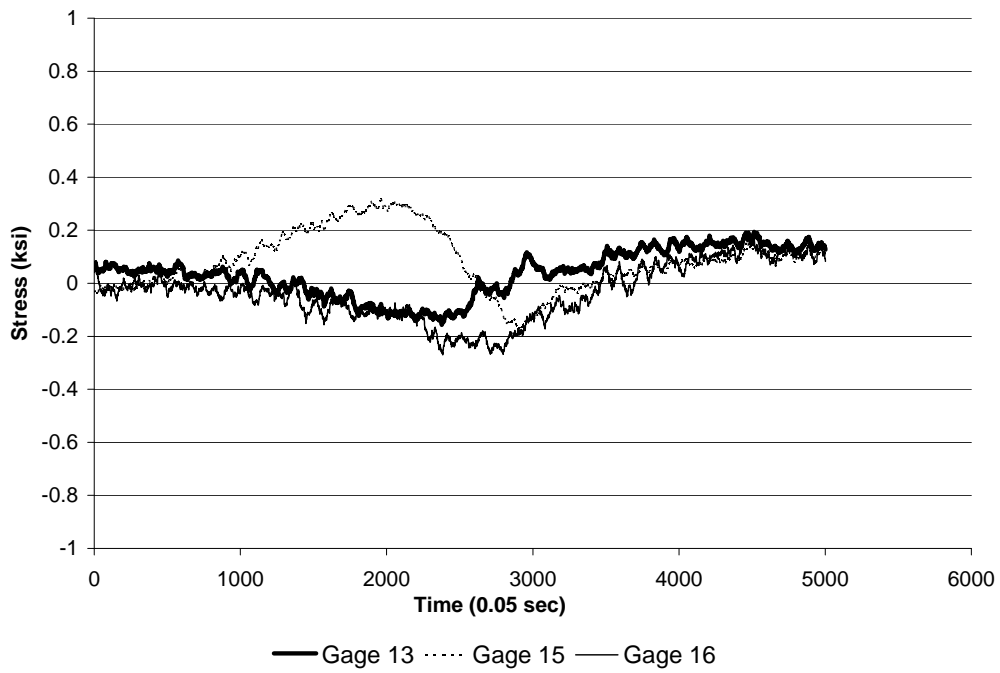
Figure D-8: Strain Gage Results Due to Truck Loading Eastbound 5 mph B
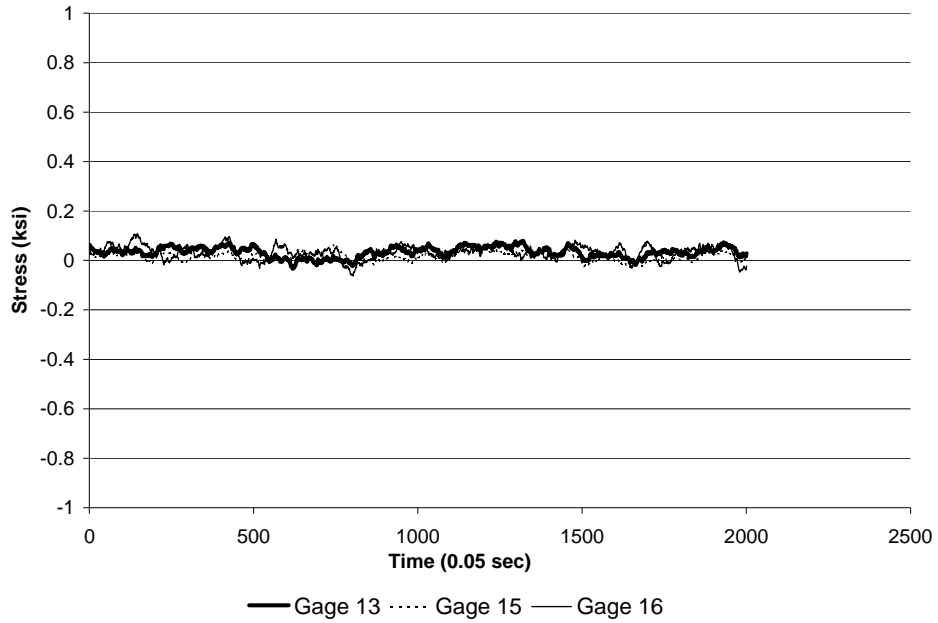
Figure D-9: Strain Gage Results Due to Truck Loading Eastbound 25 mph
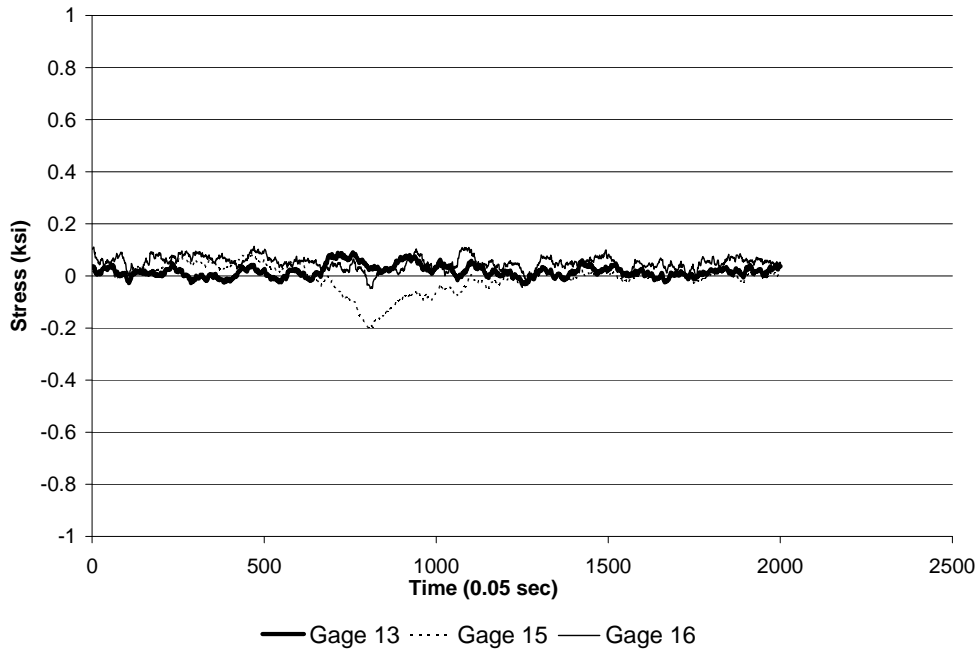
Figure D-10: Strain Gage Results Due to Truck Loading Eastbound 45 mph
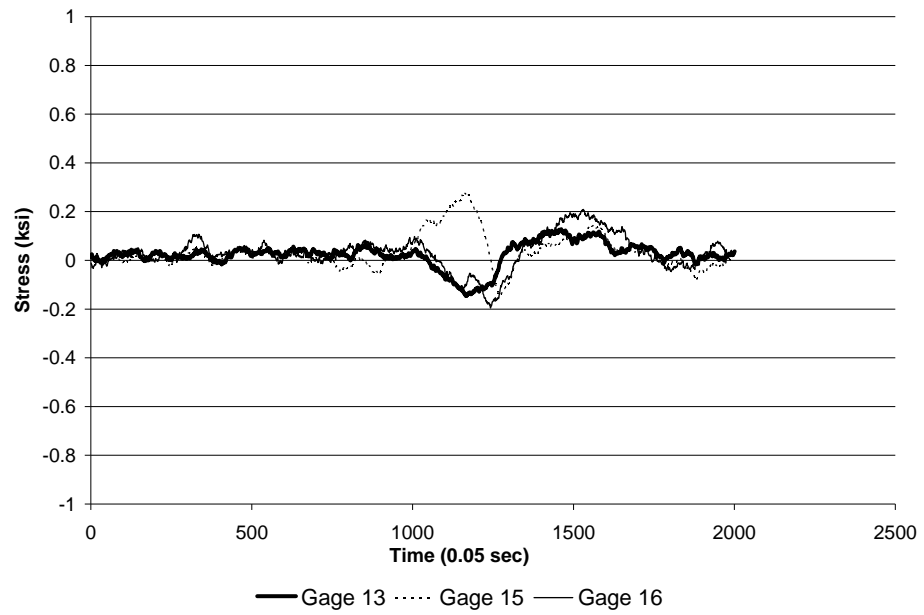
Figure D-11: Strain Gage Results Due to Truck Loading Eastbound 65 mph B

APPENDIX E   UNIQUE CRACKING

During the 2005 retrofit, unforeseen cracking occurred in the web of a girder. The crack appeared when the pin and hanger system on the bridge was being replaced. Therefore, the cracking had occurred during an unknown and unlikely loading case. Gages were placed in the area of the cracking during the post-retrofit test. This was to confirm the theory that the normal loading stress would not induce more cracking. The results of the test are shown in Table E.1. The data proves that the stress is not great enough to cause any further propagation of the cracks.

		Gage Number				
Eastbound		24	25	26	27	28
Positive Moment	Post	0.4	0.2	0.2	0.3	0.2
Negative Moment	Post	-0.2	-0.1	-0.2	-0.1	-0.2
Westbound		24	25	26	27	28
Positive Moment	Post	0.1	0.1	0.1	0.1	0.1
Negative Moment	Post	-0.1	-0.1	-0.1	-0.1	-0.1

Table E.1: Average Stress (ksi) for Gages near the Unique Cracking.

APPENDIX F   LONGITUDINAL STIFFENER REPORT

a. Summary:

The results of a study investigating the stress distribution at the termination of a longitudinal stiffener in a web girder are presented. Two different configurations were investigated. The first configuration represents the stiffener in the as-built condition, while the second configuration corresponds to the stiffener after a proposed repair. A comparison of the local stresses induced by the two configurations was carried out using finite element models. The software used to carry out the analyses was ABAQUS V 6.4-1. It was found that the repaired configuration had peak stresses that were approximately 25% lower than the as-build configuration. In addition, the stress gradient along the stiffener was found to be more gradual for the repaired configuration, and distributed over a larger area.

b. Table of contents:

c. List of Figures:

1. **Material specs:**

It was assumed that the girder web, weld material, and the stiffener had the same material properties (linear-elastic steel).

2. Analysis, boundary conditions and applied load:

The finite element model consisted of a segment of girder with a stiffener attached to it. The type of analysis performed was linear-elastic. As shown in Figures 3 and 8, a uniform stress of 36 ksi was applied at the end of the model where the stiffener was present. The model was restrained from motion at the opposite end. Displacements were restrained in the x direction in all nodes of this end of the model. In addition, the motion in the z direction was restrained for all nodes located in bottom row.

3. Geometry: "Before Repair"
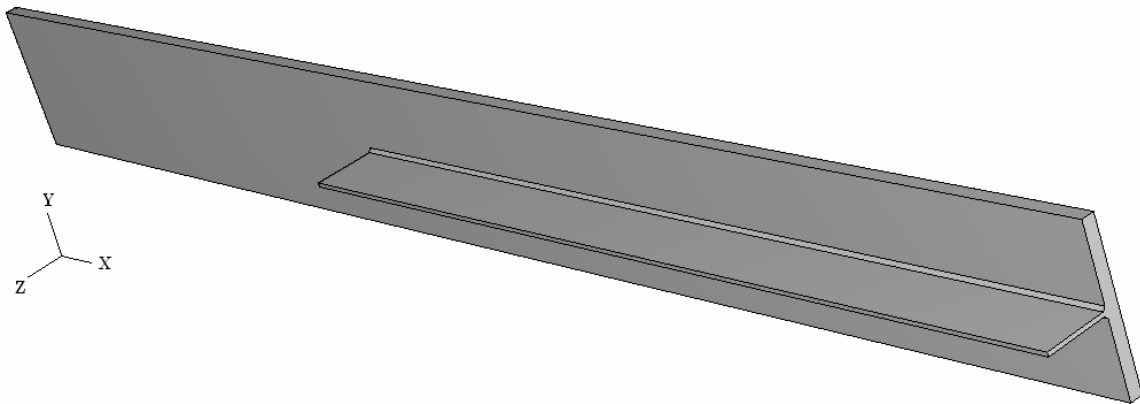
Figure 1 – Axis orientation - before repair.
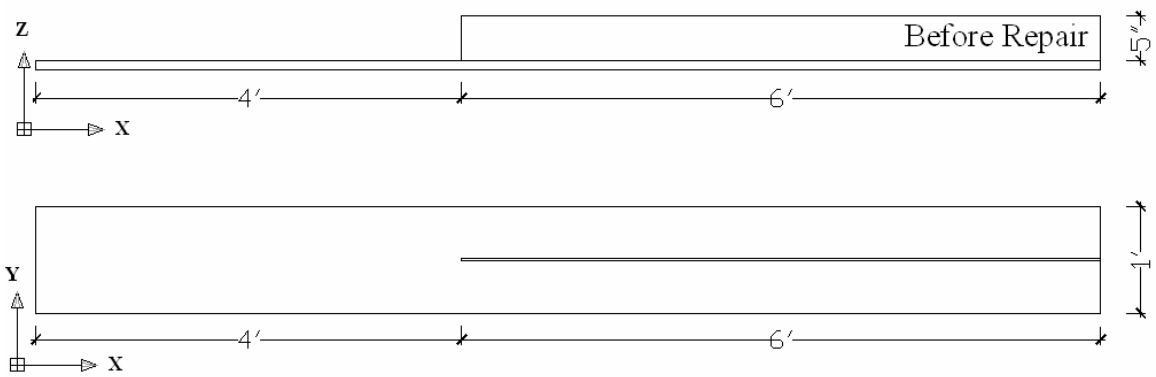
Figure 2 – Dimensions – before repair.

4. Boundary Conditions and Loads: "Before Repair"
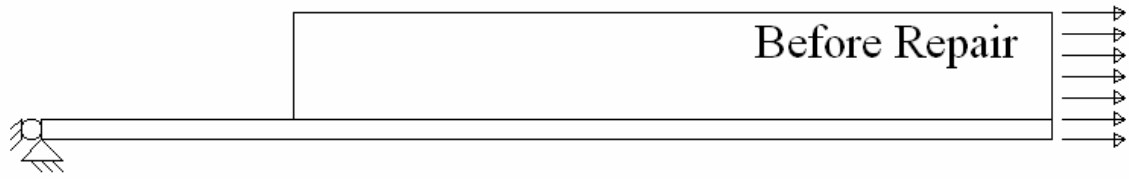
Figure 3 – Boundary conditions and applied stresses – before repair.

5. Mesh: "Before Repair"
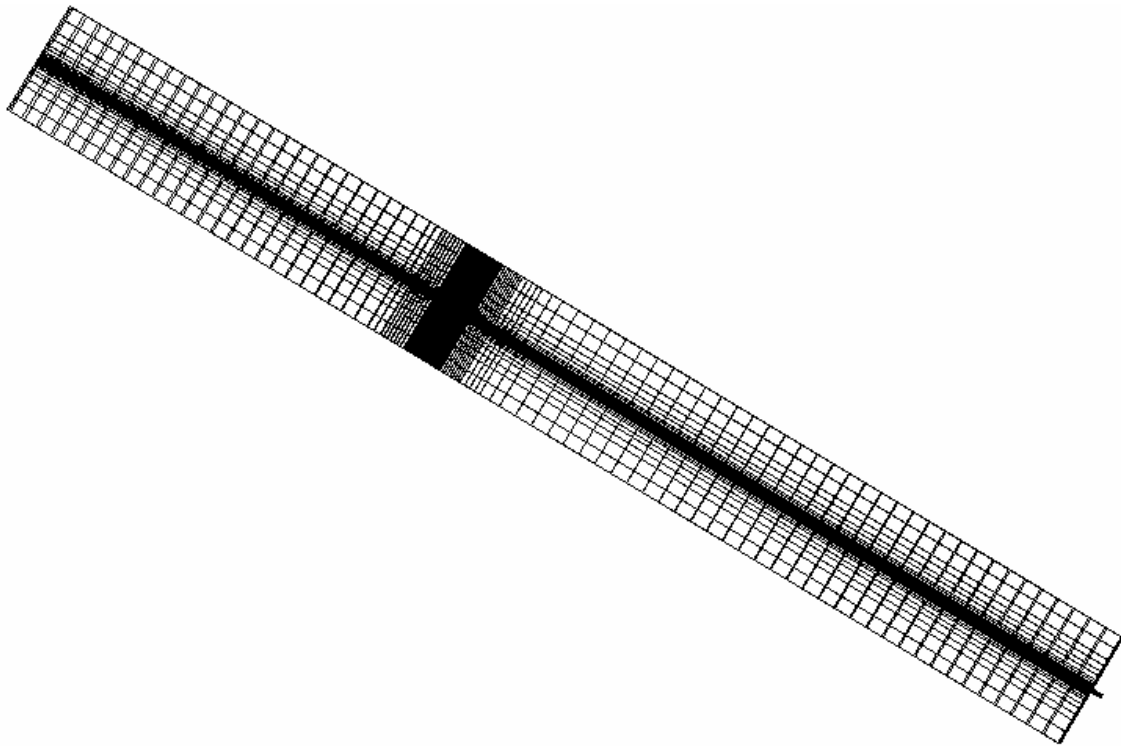
Figure 4 – Mesh (x-y) – before repair.
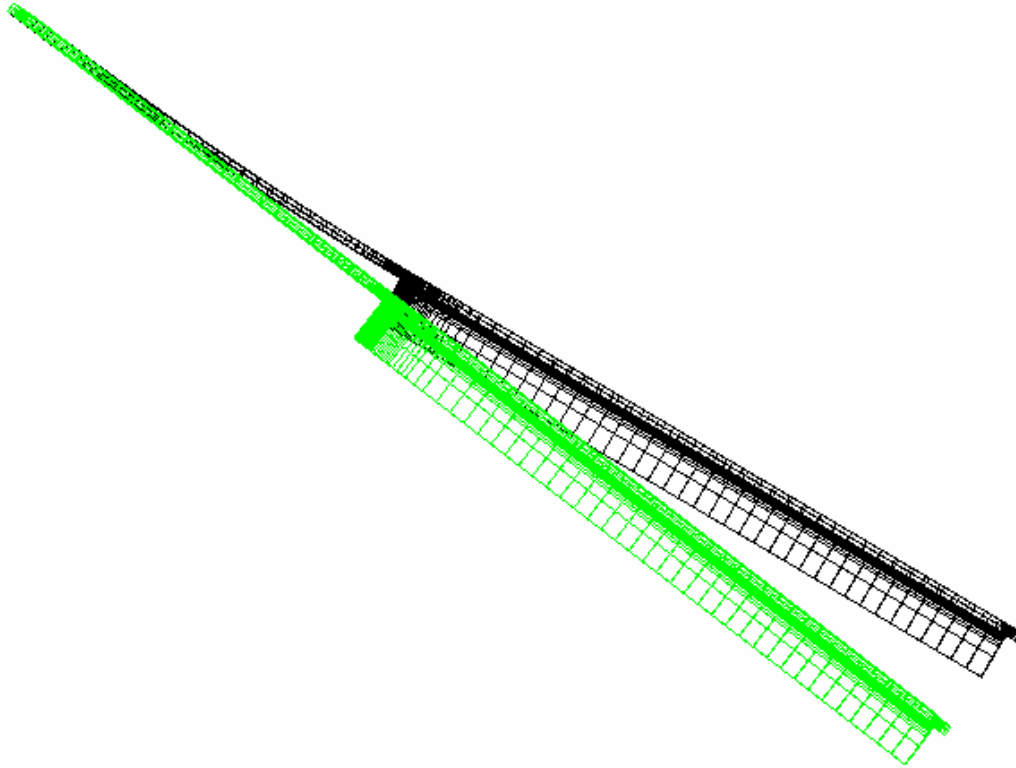
Figure 5 – Superimposed deformed and undeformed configurations (x-z) – before repair.

6. Geometry: "After Repair"
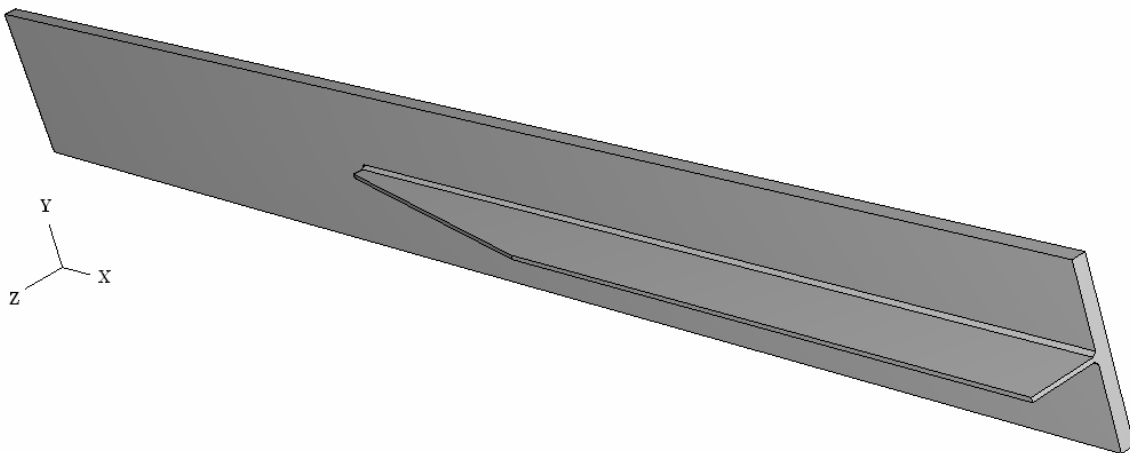
Figure 6 – Axis orientation - after repair.
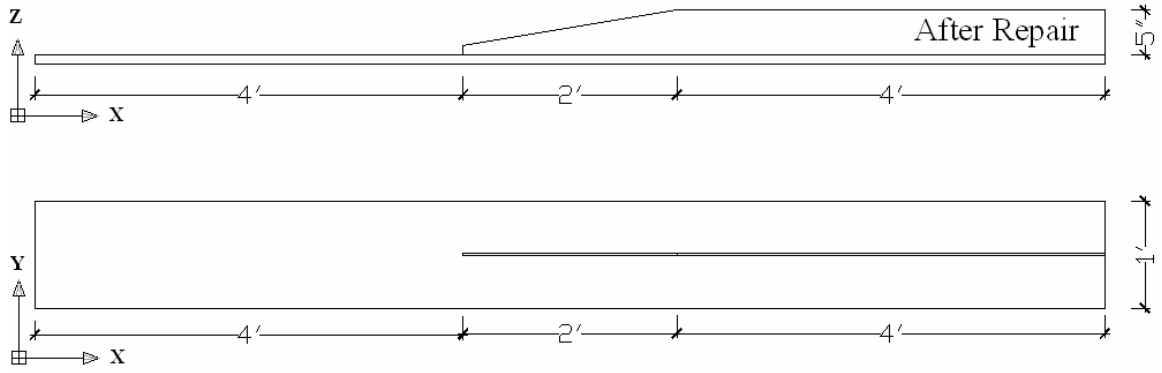
Figure 7 – Dimensions – after repair.

7. Boundary Conditions and Loads: "After Repair"
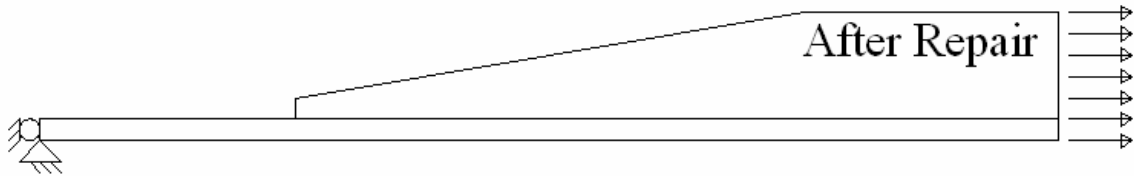
Figure 8 – Boundary conditions and applied stresses – after repair.

8. Mesh: "After Repair"
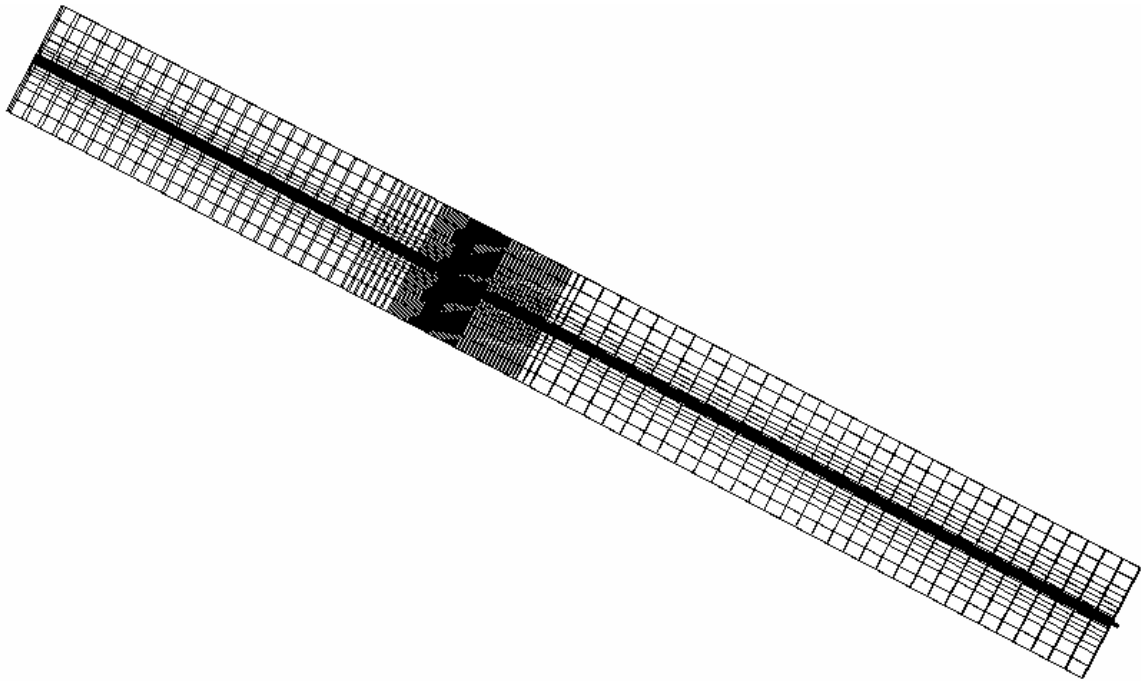
Figure 9 – Mesh (x-y) – after repair.
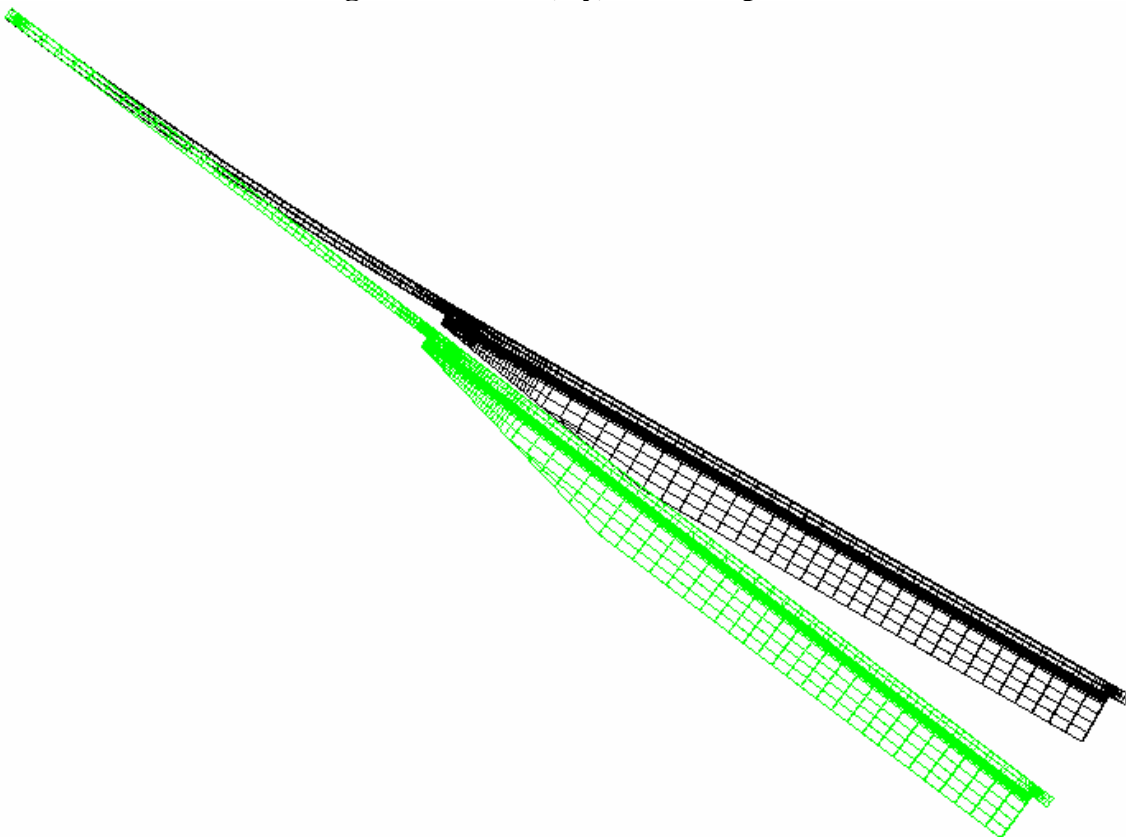
Figure 10 – Superimposed deformed and undeformed configurations (x-z) – after repair.

9. FEM results:
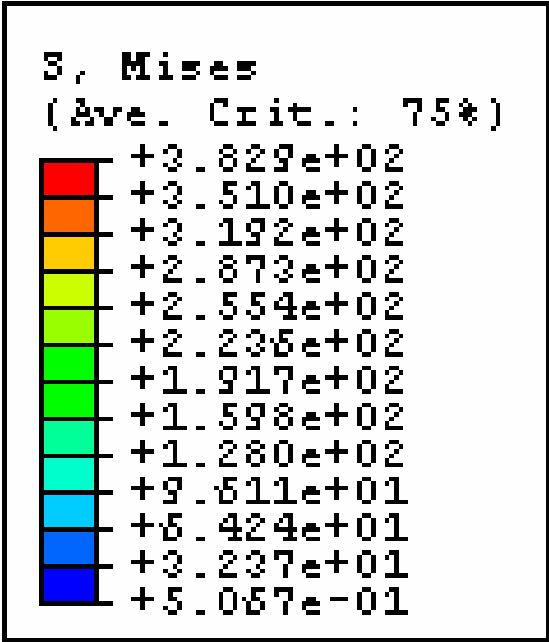
Figure 11 – Stress scale.
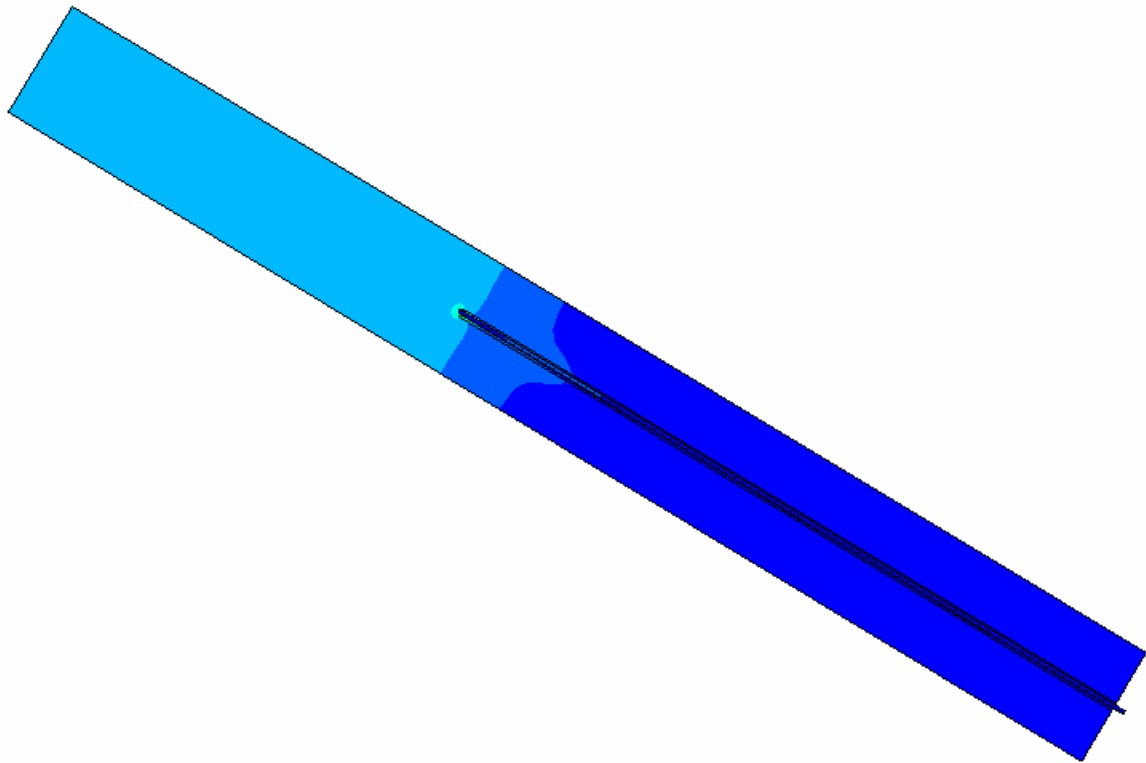
Figure 12 - Girder web/stiffener (x-y) – before repair.
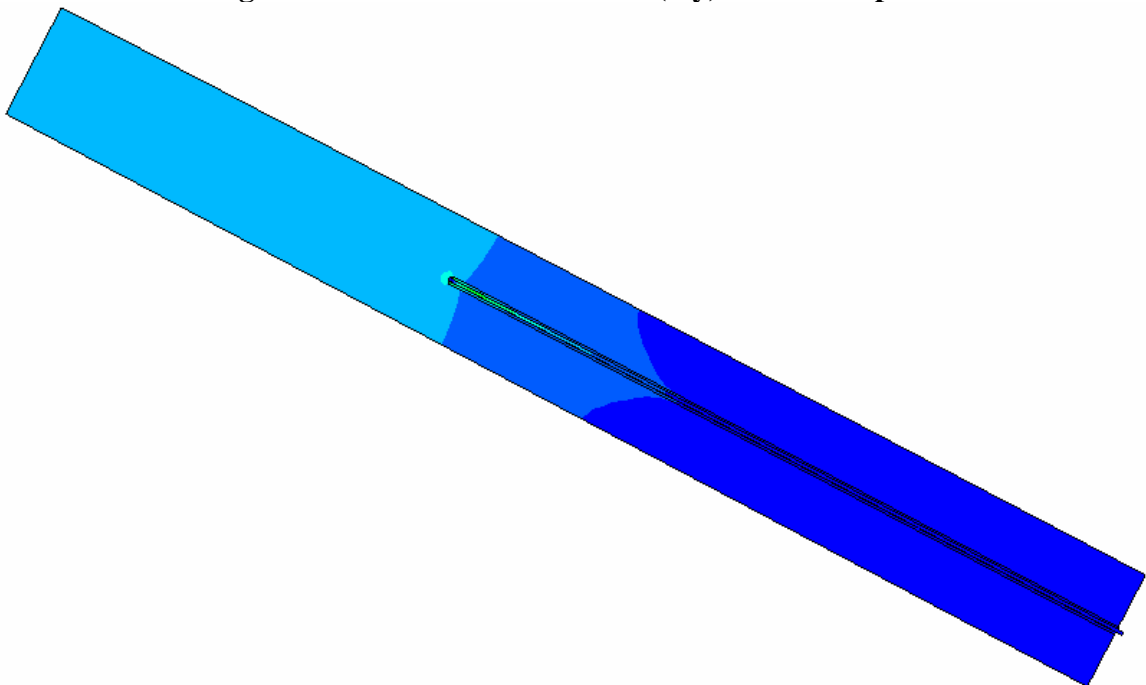
Figure 13 - Girder web/stiffener (x-y) – after repair.
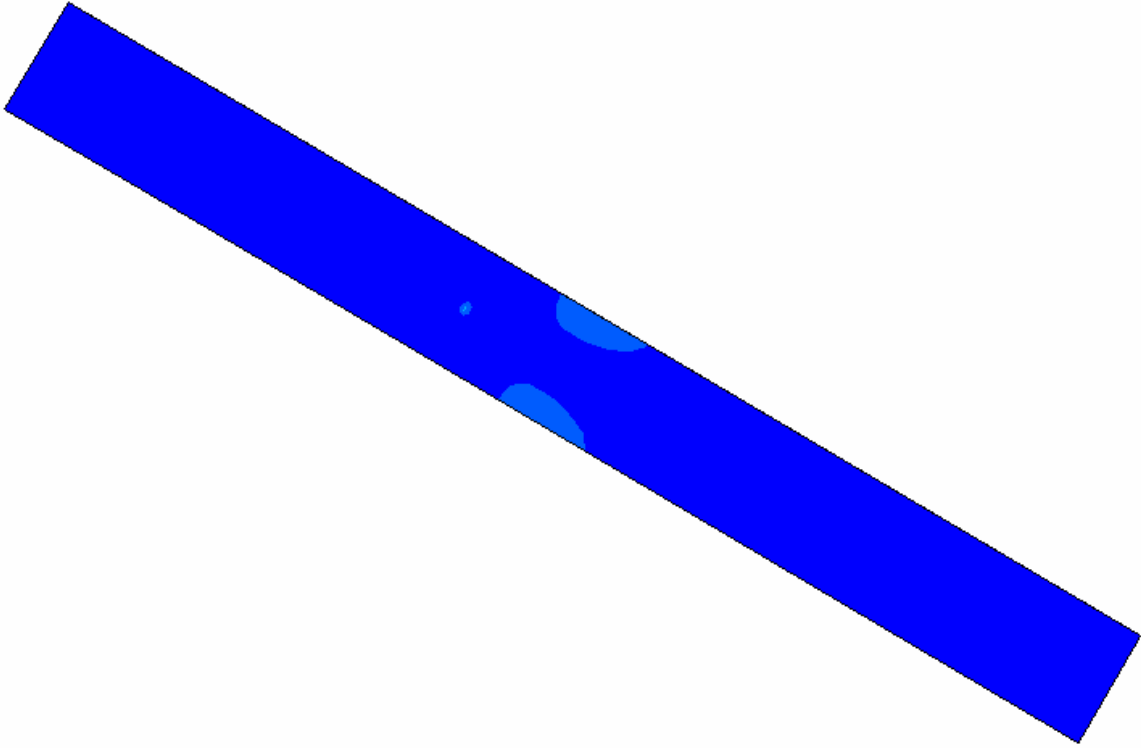
Figure 14 - Girder web (x-y) - before repair.
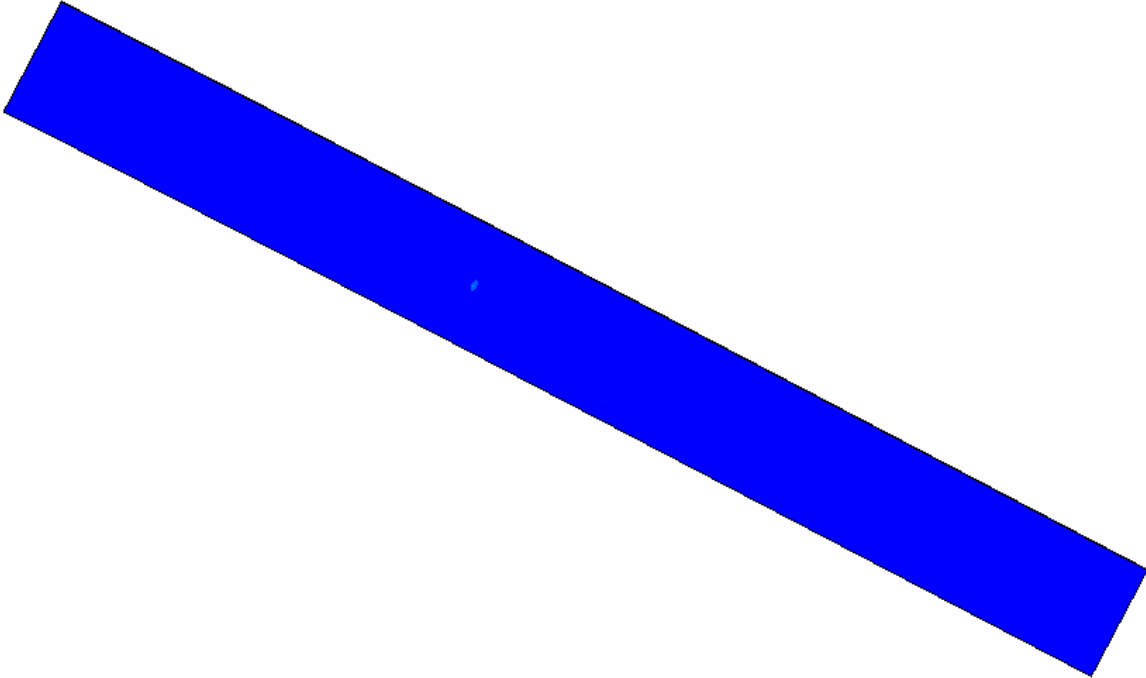
Figure 15 - Girder web (x-y) - after repair.
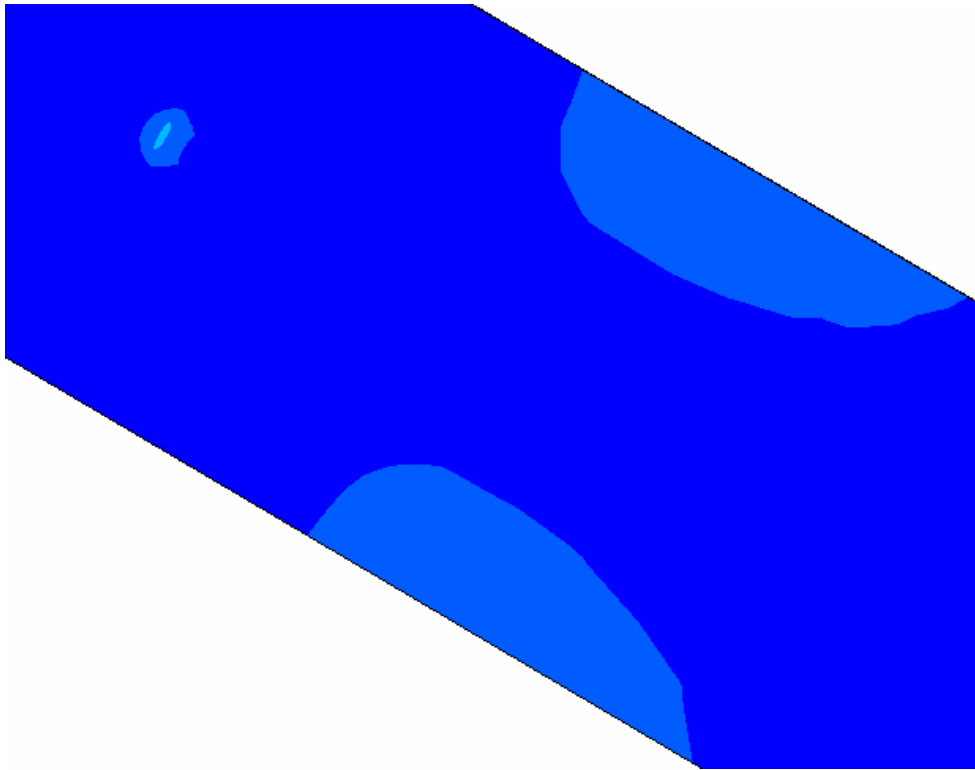
Figure 16 - Girder web (x-y) - detail 1 - before repair.
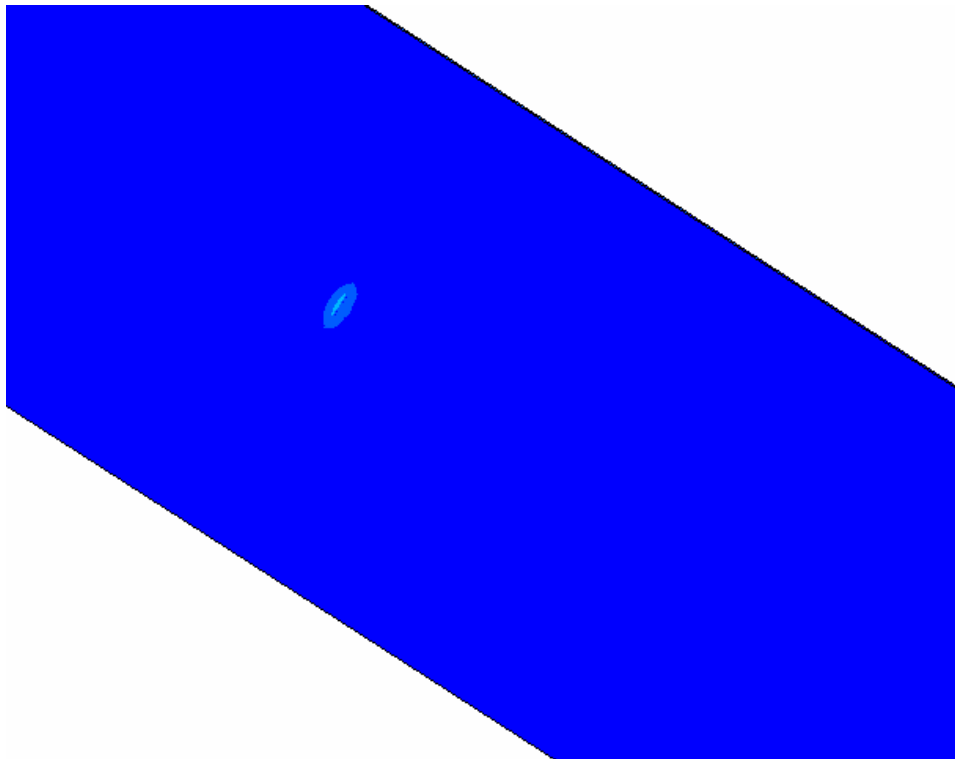
Figure 17 - Girder web (x-y) - detail 1- after repair.
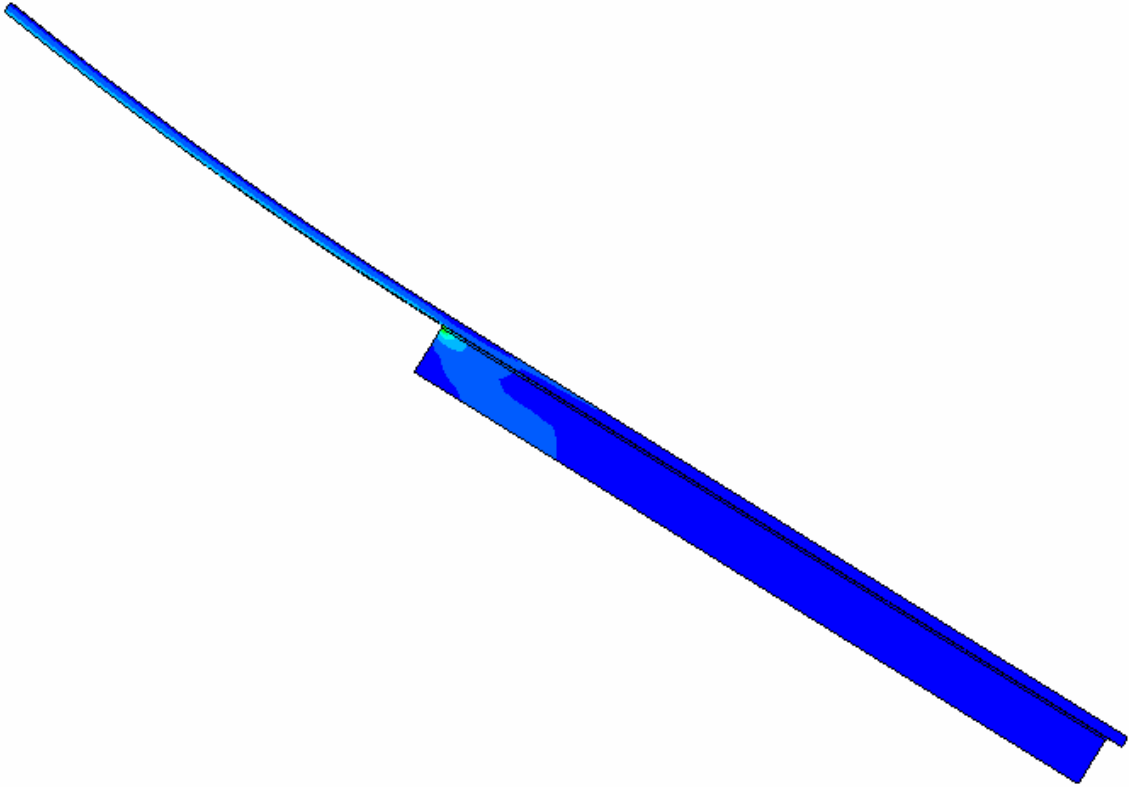
Figure 18 - Stiffener (x-z) – before repair.
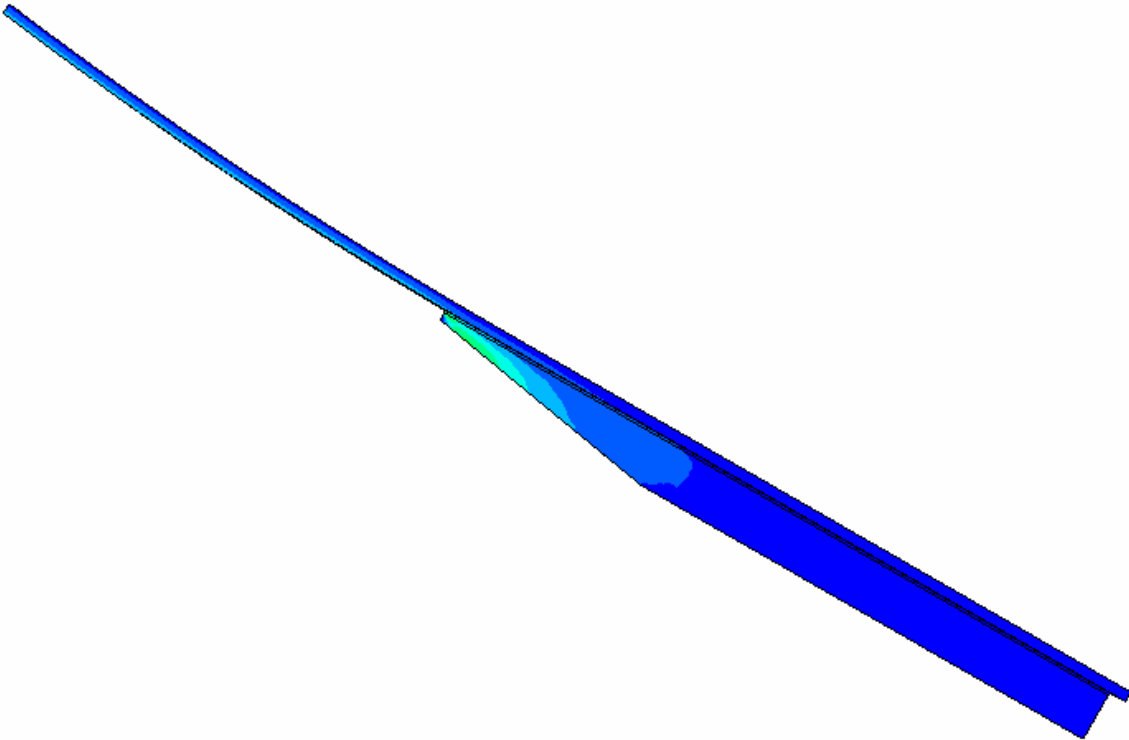
Figure 19 - Stiffener (x-z) – after repair.

73
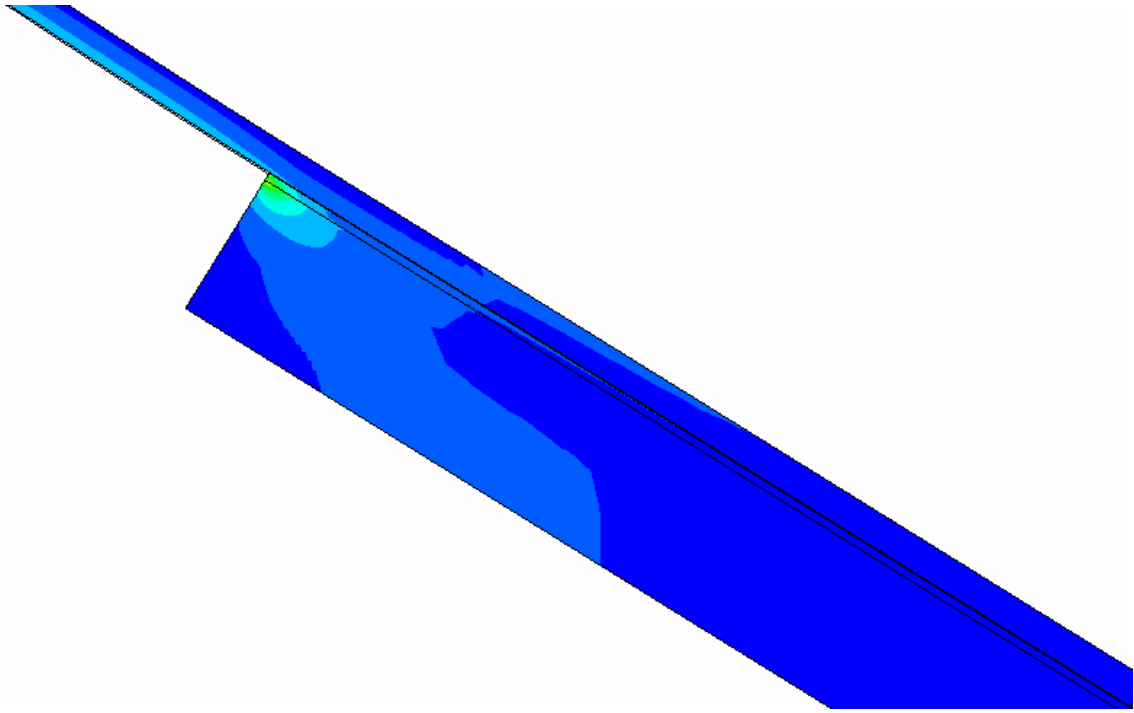
Figure 20 - Stiffener (x-z) – detail 1 – before repair.
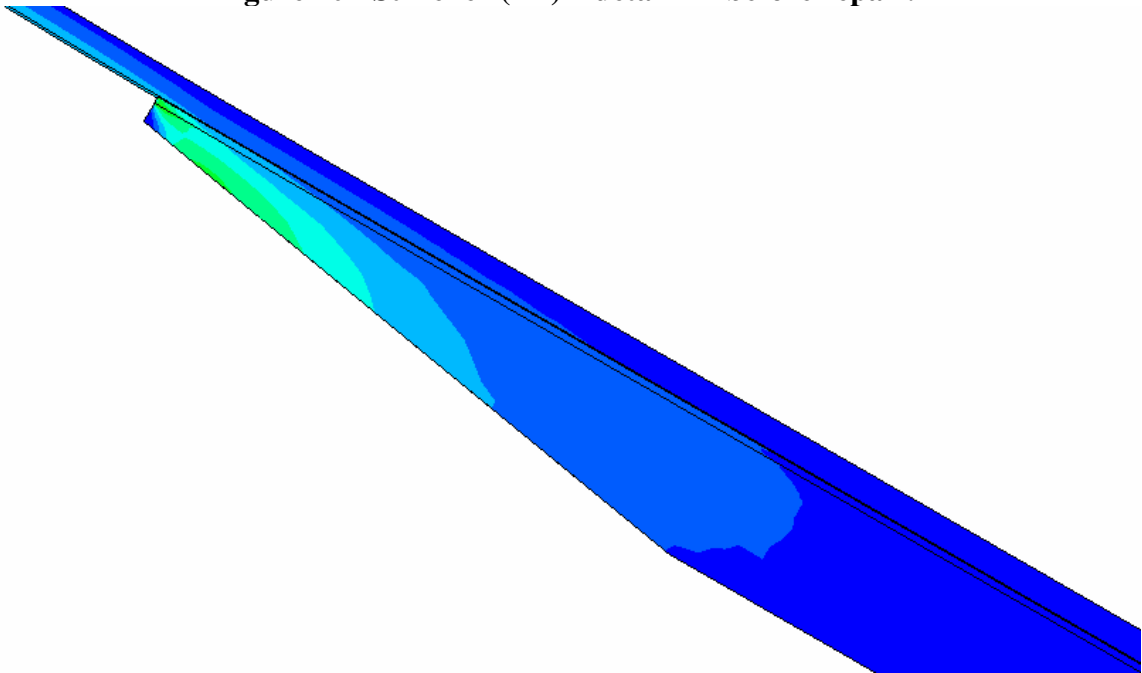
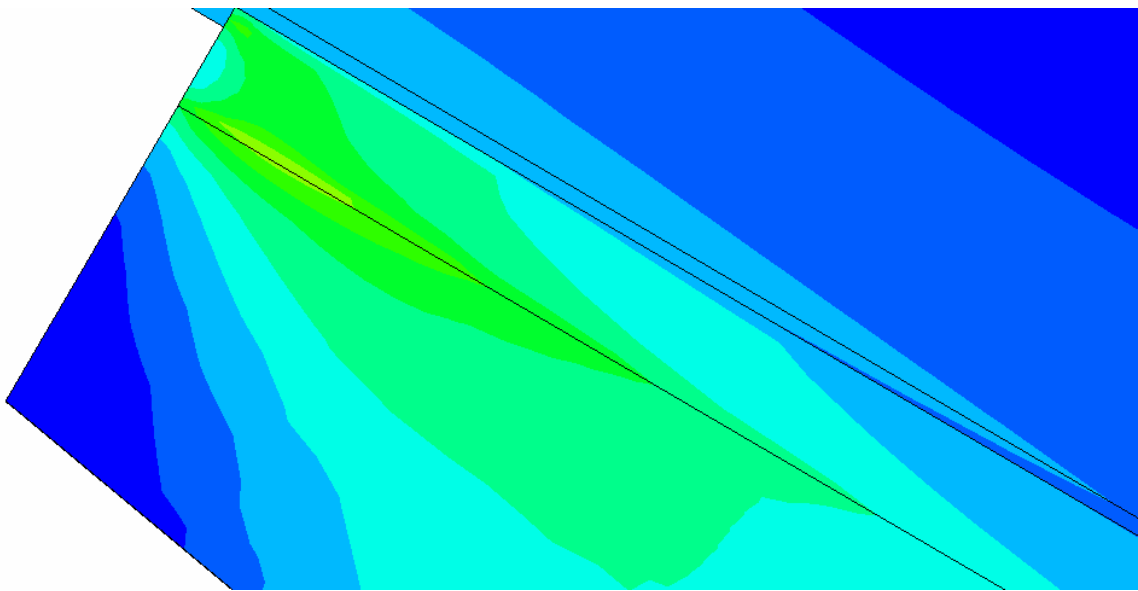**Figure 21 - Stiffener (x-z) – detail 1 – after repair.**
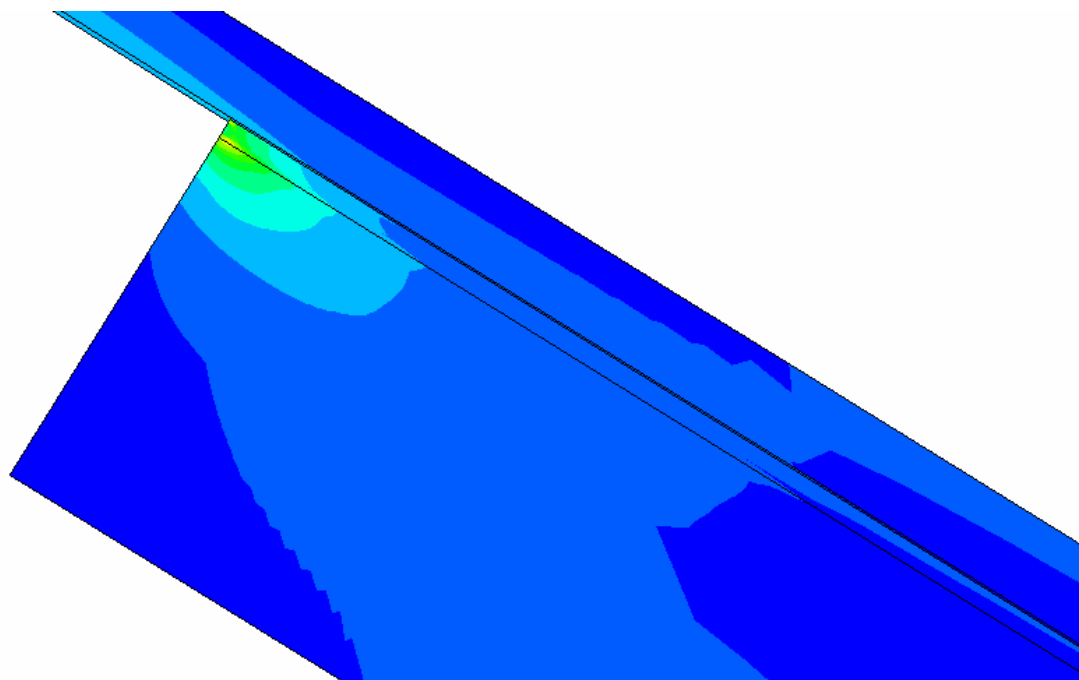
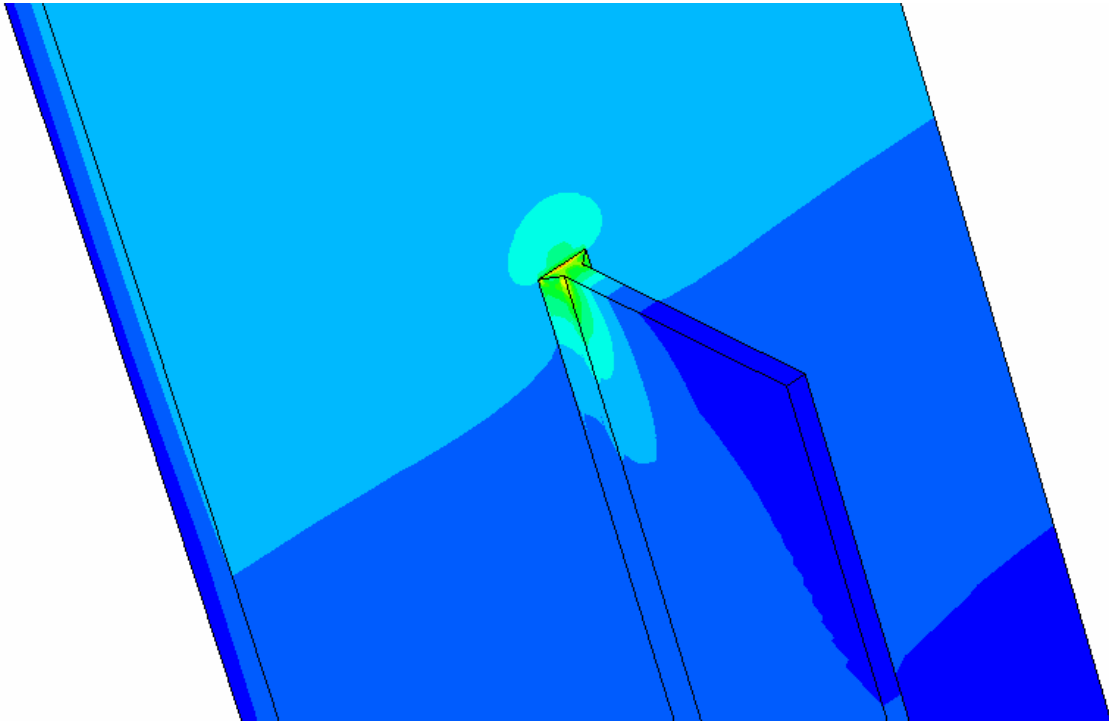**Figure 22- Stiffener (x-z) – detail 2 – before repair.**
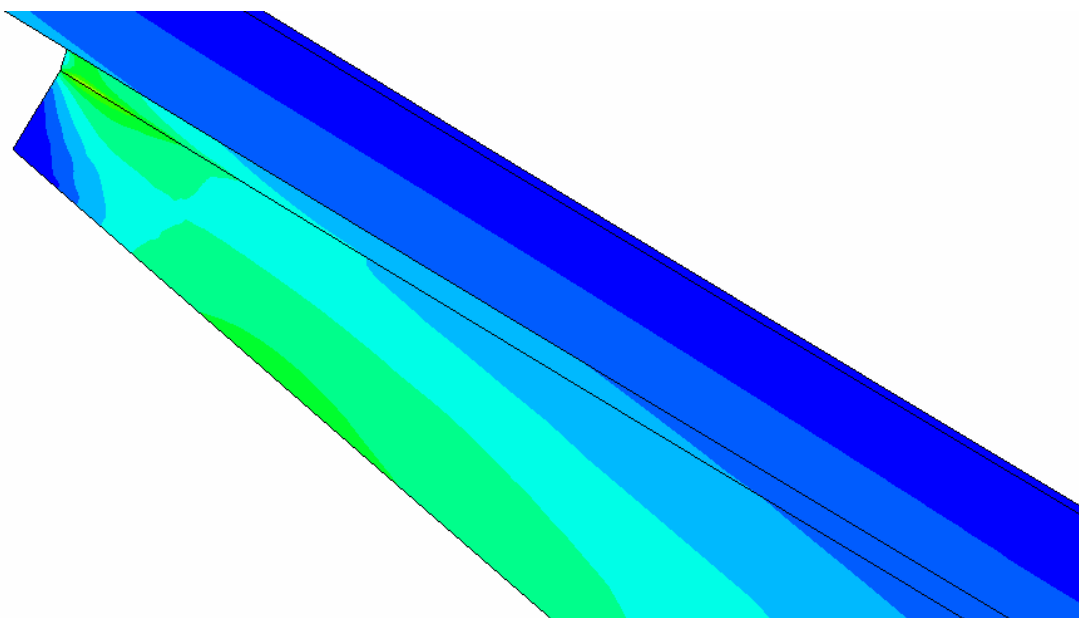
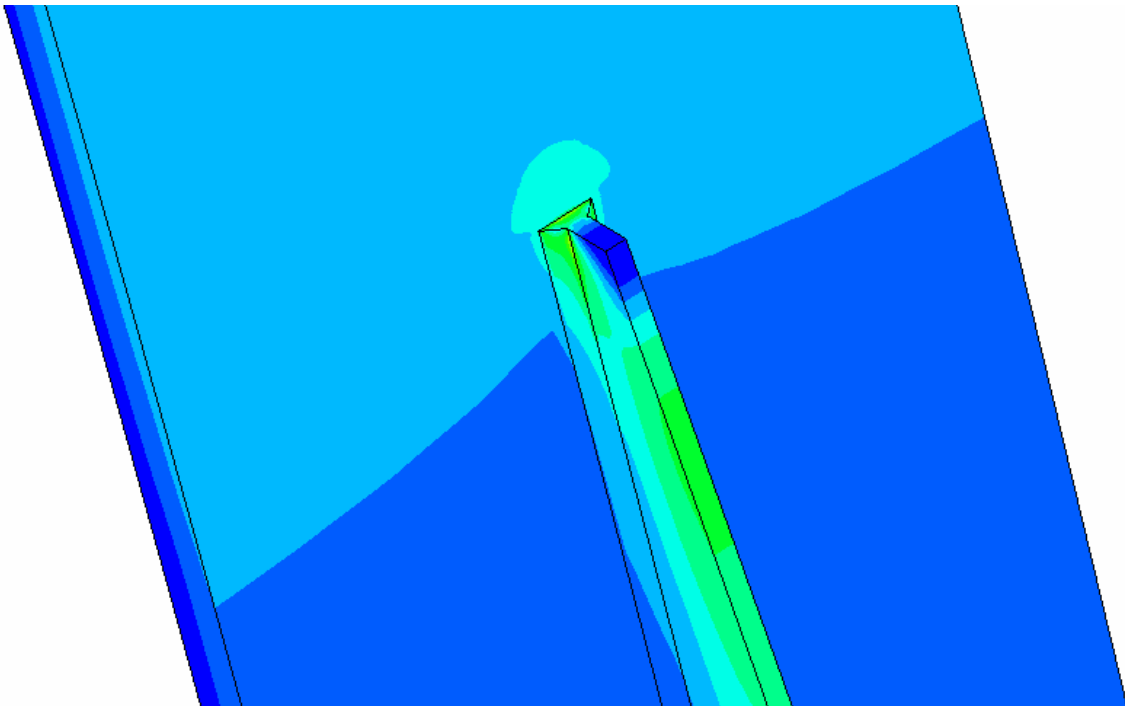**Figure 23 - Stiffener (x-z) – detail 2 – after repair.**
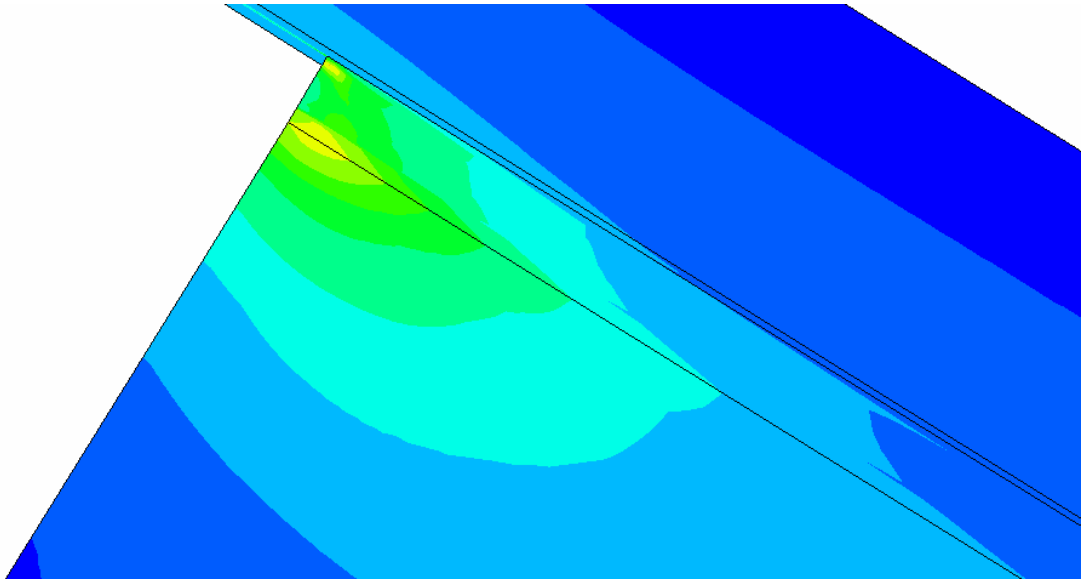
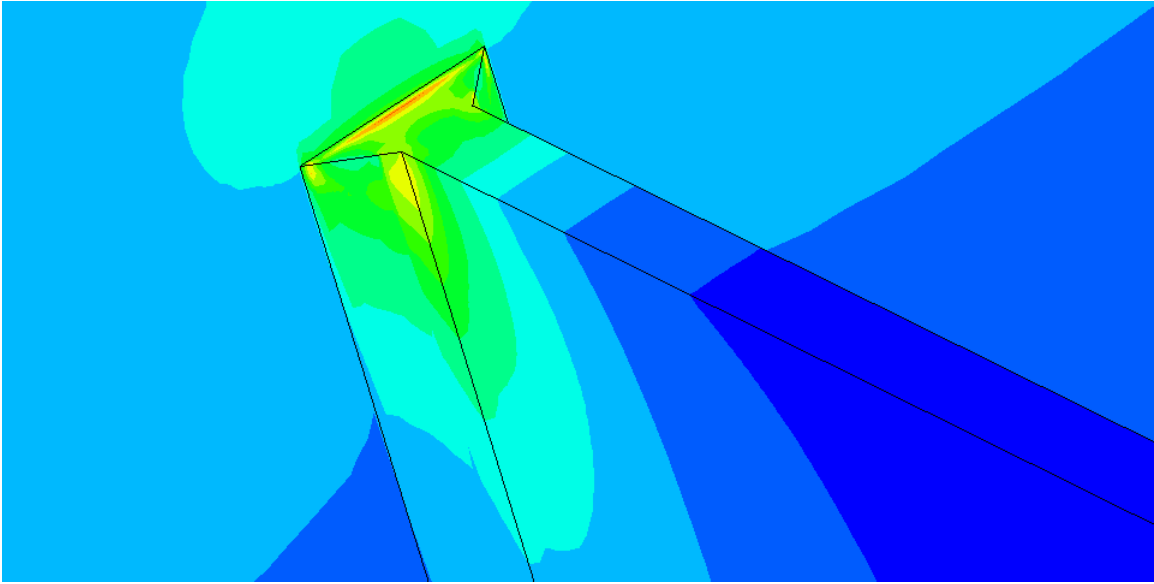**Figure 24 - Stiffener (x-z) – detail 3 – before repair.**

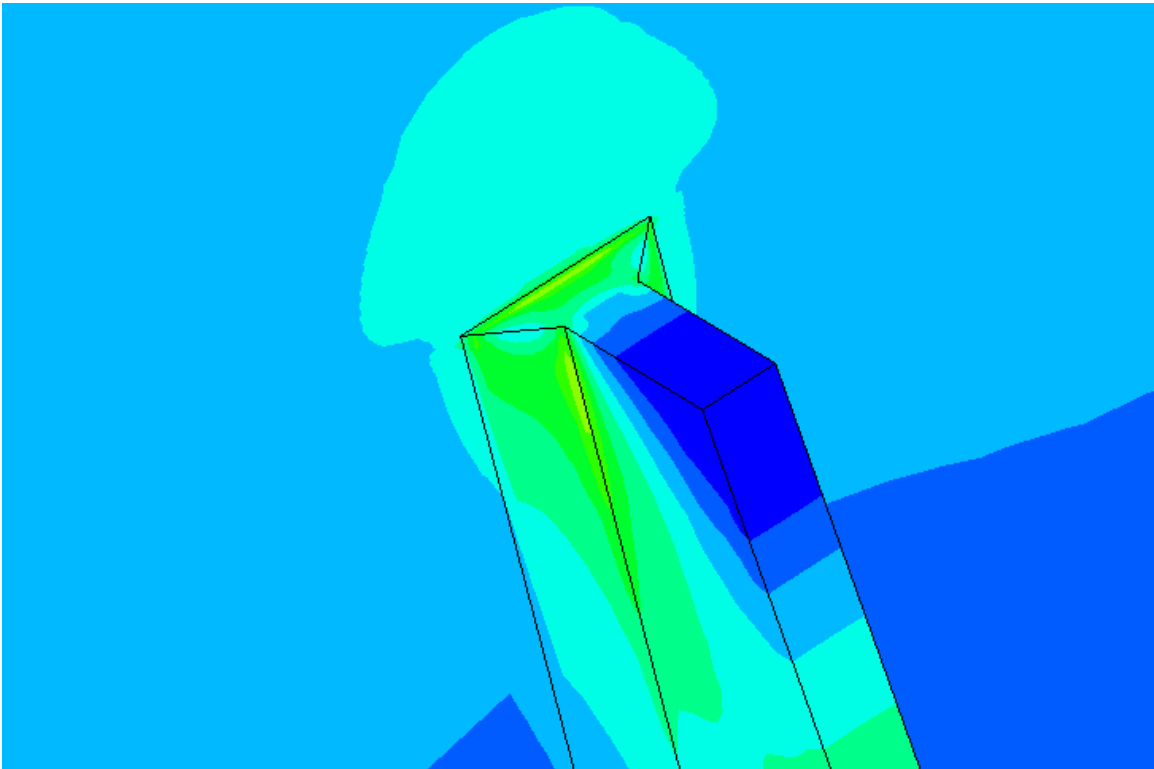**Figure 25 - Stiffener (x-z) – detail 3 – after repair.**

76

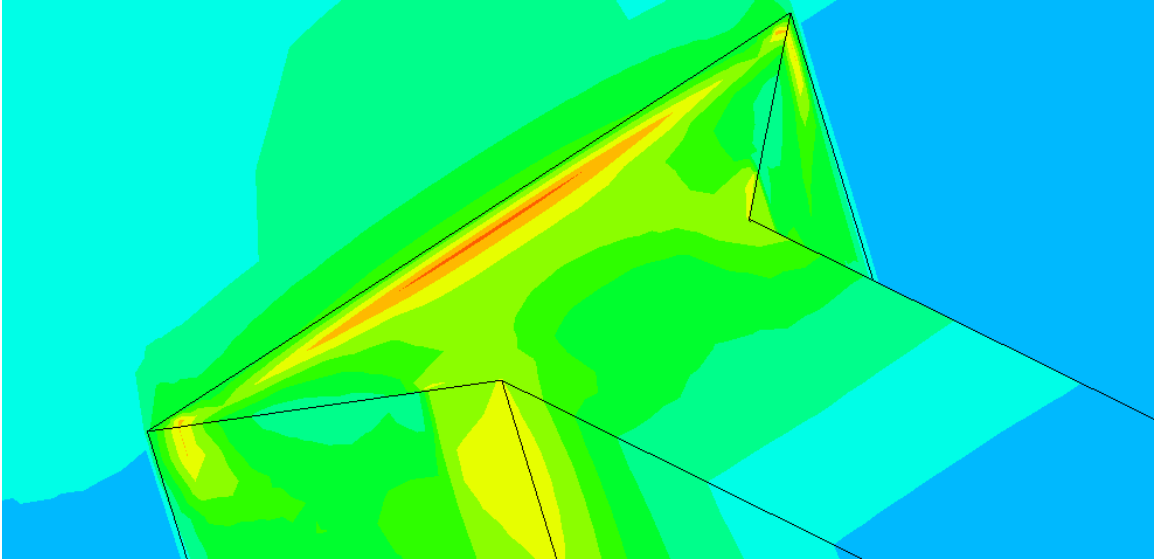**Figure 26 – Tip of stiffener - detail 1- before repair.**

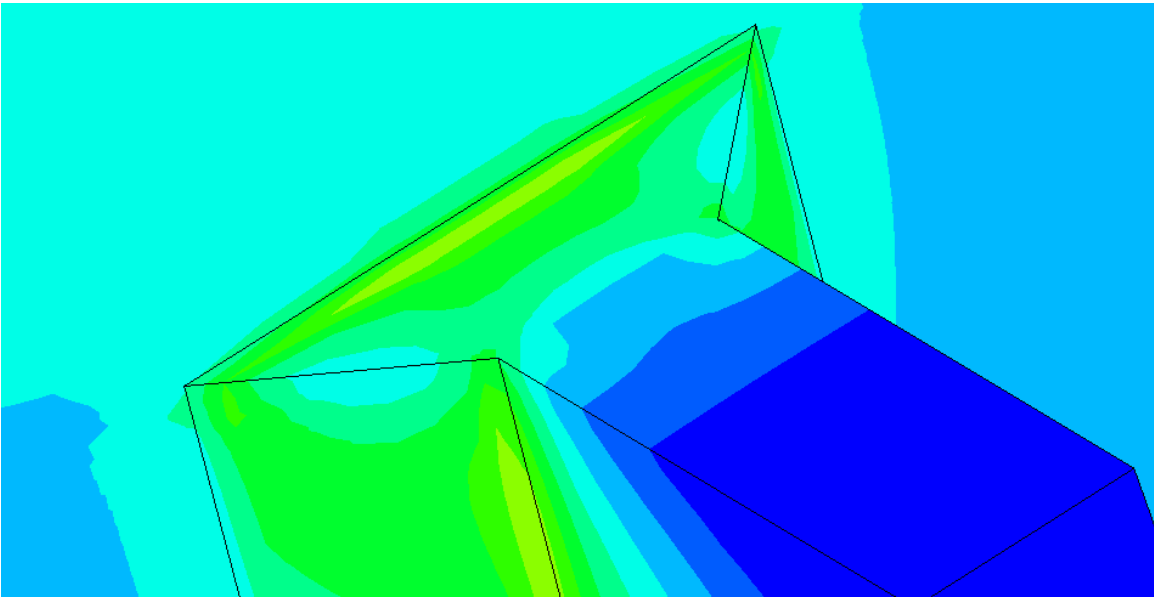**Figure 27 – Tip of stiffener - detail 1- after repair.**

Figure 28 – Tip of stiffener - detail 2- before repair.

Figure 29 – Tip of stiffener - detail 2- after repair.

Figure 30 – Tip of stiffener –detail 3- before repair.

Figure 31 – Tip of stiffener –detail 3- after repair.

10. Results comments:

Figures 12 and 13 show that reduction in the stresses along the girder web caused by the repair was not significant. Although stress concentrations were localized at the tip of the stiffener in both cases, the maximum stress decreased after the repair.

Figures 14 thru 17 show that on the side of the girder web opposite to the stiffener, stress concentrations were found right at the tip of the stiffener. However, the area over which these stress concentrations were present was very small. The implementation of the proposed repair did reduce the size of the region affected by stress concentrations. The FEM indicate that stress gradients at the sides of the model, near the tip of the stiffener, were eliminated by the repair (Figures 14 through 17).

Figures 18 through 25 show that the longitudinal stresses along the stiffener were similar in magnitude. After the repair, stresses propagated from the tip of the stiffener over a larger area along the stiffener. Also the stress distribution after the repair shows a much more gradual gradient. This can be observed in Figures 24 and 25 (detail 3), where areas with higher stresses are shown in yellow.

Figures 26 thru 31 show that the magnitude of the stresses (shown in increasing order of magnitude as yellow, orange and red) decreased with the repair. Figures 30 and 31 show that the front face of the stiffener within the fillet weld region was the area most affected by these stress concentrations. It was found by direct comparison of results from FEMs that after the repair the maximum stresses were reduced by approximately 25%, which would improve the fatigue life.